

Spike-and-Slab Group Lassos for Grouped Regression and Sparse Generalized Additive Models

Ray Bai^{*†}, Gemma E. Moran^{‡§}, Joseph L. Antonelli^{¶||},
Yong Chen^{*}, Mary R. Boland^{*}

December 15, 2024

Abstract

We introduce the spike-and-slab group lasso (SSGL) for Bayesian estimation and variable selection in linear regression with grouped variables. We further extend the SSGL to sparse generalized additive models (GAMs), thereby introducing the first nonparametric variant of the spike-and-slab lasso methodology. Our model simultaneously performs group selection and estimation, while our fully Bayes treatment of the mixture proportion allows for model complexity control and automatic self-adaptivity to different levels of sparsity. We develop theory to uniquely characterize the global posterior mode under the SSGL and introduce a highly efficient block coordinate ascent algorithm for maximum a posteriori (MAP) estimation. We further employ de-biasing methods to provide uncertainty quantification of our estimates. Thus, implementation of our model avoids the computational intensiveness of Markov chain Monte Carlo (MCMC) in high dimensions. We derive posterior concentration rates for both grouped linear regression and sparse GAMs when the number of covariates grows at nearly exponential rate with sample size. Finally, we illustrate our methodology through extensive simulations and data analysis.

^{*}Department of Biostatistics, Epidemiology, and Informatics, University of Pennsylvania, Philadelphia, PA 19104.

[†]Co-first author. Email: Ray.Bai@pennmmedicine.upenn.edu

[‡]Data Science Institute, Columbia University, New York, NY 10027.

[§]Co-first author. Email: gm2918@columbia.edu

[¶]Department of Statistics, University of Florida, Gainesville, FL 32611.

^{||}Co-first author. Email: jantonelli@ufl.edu

1 Introduction

1.1 Regression with Grouped Variables

Group structure arises in many statistical applications. For example, in multifactor analysis of variance, multi-level categorical predictors are each represented by a group of dummy variables. In genomics, genes within the same pathway may form a group at the pathway or gene set level and act in tandem to regulate a biological system. In each of these scenarios, the response $\mathbf{Y}_{n \times 1}$ can be modeled as a linear regression problem with G groups:

$$\mathbf{Y} = \sum_{g=1}^G \mathbf{X}_g \boldsymbol{\beta}_g + \boldsymbol{\varepsilon}, \quad (1.1)$$

where $\boldsymbol{\varepsilon} \sim \mathcal{N}_n(\mathbf{0}, \sigma^2 \mathbf{I}_n)$, $\boldsymbol{\beta}_g$ is a coefficients vector of length m_g , and \mathbf{X}_g is an $n \times m_g$ covariate matrix corresponding to group $g = 1, \dots, G$. Even in the absence of grouping information about the covariates, the model (1.1) subsumes a wide class of important nonparametric regression models called *generalized additive models* (GAMs). In GAMs, continuous covariates may be represented by groups of basis functions which have a nonlinear relationship with the response. We defer further discussion of GAMs to Section 5.

It is often of practical interest to select groups of variables that are most significantly associated with the response. To facilitate this group-level selection, Yuan and Lin [53] introduced the group lasso, which solves the optimization problem,

$$\arg \min_{\boldsymbol{\beta}} \frac{1}{2} \left\| \mathbf{Y} - \sum_{g=1}^G \mathbf{X}_g \boldsymbol{\beta}_g \right\|_2^2 + \lambda \sum_{g=1}^G \sqrt{m_g} \|\boldsymbol{\beta}_g\|_2, \quad (1.2)$$

where $\|\cdot\|_2$ is the ℓ_2 norm. In the frequentist literature, many variants of model (1.2) have been introduced, which use some combination of ℓ_1 and ℓ_2 penalties on the coefficients of interest (e.g., [16, 20, 39]).

In the Bayesian framework, selection of relevant groups under model (1.1) is often done by placing spike-and-slab priors on each of the groups $\boldsymbol{\beta}_g$ (e.g., [49, 24, 50, 30]). These priors typically take the form,

$$\begin{aligned} \pi(\boldsymbol{\beta}|\boldsymbol{\gamma}) &= \prod_{g=1}^G [(1 - \gamma_g) \delta_0(\boldsymbol{\beta}_g) + \gamma_g \pi(\boldsymbol{\beta}_g)], \\ \pi(\boldsymbol{\gamma}|\theta) &= \prod_{g=1}^G \theta^{\gamma_g} (1 - \theta)^{1 - \gamma_g}, \\ \theta &\sim \pi(\theta), \end{aligned} \quad (1.3)$$

where γ is a binary vector that indexes the 2^G possible models, $\theta \in (0, 1)$ is the mixing proportion, δ_0 is a point mass at $\mathbf{0}_{m_g} \in \mathbb{R}^{m_g}$ (the “spike”), and $\pi(\beta_g)$ is an appropriate “slab” density (typically a multivariate normal distribution or a scale-mixture multivariate normal density). With a well-chosen prior on θ , this model will favor parsimonious models in very high dimensions, thus avoiding the curse of dimensionality.

1.2 The Spike-and-Slab Lasso

For Bayesian variable selection, point mass spike-and-slab priors (1.3) are interpretable, but they are computationally intractable in high dimensions, due in large part to the combinatorial complexity of updating the discrete indicators γ . As an alternative, fully continuous variants of spike-and-slab models have been developed. For continuous spike-and-slab models, the point mass spike δ_0 is replaced by a continuous density heavily concentrated around $\mathbf{0}_{m_g}$. This not only mimics the point mass but it *also* facilitates more efficient computation, as we describe later.

In the context of sparse normal means estimation and univariate linear regression, Ročková [34] and Ročková and George [36] introduced the spike-and-slab lasso (SSL). The SSL places a mixture prior of two Laplace densities on the individual coordinates β_j , i.e.

$$\pi(\beta|\theta) = \prod_{j=1}^p [(1 - \theta)\psi(\beta_j|\lambda_0) + \theta\psi(\beta_j|\lambda_1)], \quad (1.4)$$

where $\theta \in (0, 1)$ is the mixing proportion and $\psi(\cdot|\lambda)$ denotes a univariate Laplace density indexed by hyperparameter λ , i.e. $\psi(\beta|\lambda) = \frac{\lambda}{2}e^{-\lambda|\beta|}$. Typically, we set $\lambda_0 \gg \lambda_1$ so that the spike is heavily concentrated about zero. Unlike (1.3), the SSL model (1.4) does not place any mass on exactly sparse vectors. Nevertheless, the global posterior mode under the SSL prior may be exactly sparse. Meanwhile, the slab stabilizes posterior estimates of the larger coefficients so they are not downward biased. Thus, the SSL posterior mode can be used to perform variable selection and estimation simultaneously.

The spike-and-slab lasso methodology has now been adopted for a wide number of statistical problems. Apart from univariate linear regression, it has been used for factor analysis [35, 28], multivariate regression [9], covariance/precision matrix estimation [9, 11, 21], causal inference [2], generalized linear models (GLMs) [44, 42], and Cox proportional hazards models [43].

While the SSL (1.4) induces sparsity on individual coefficients (through the posterior mode), it does not account for group structure of covariates.

For inference with structured data in GLMs, Tang et al. [42] utilized the univariate spike-and-slab lasso prior (1.4) for grouped data where each group had a group-specific sparsity-inducing parameter, θ_g , instead of a single θ for all coefficients. However, this univariate SSL prior does not feature the “all in, all out” selection property of the original group lasso of Yuan and Lin [53] or the *grouped* SSL prior, which we develop in this work.

In this paper, we introduce the *spike-and-slab group lasso* (SSGL) for Bayesian grouped regression and variable selection. Under the SSGL prior, the global posterior mode is exactly sparse, thereby allowing the mode to automatically threshold out insignificant groups of coefficients. To widen the use of spike-and-slab lasso methodology for situations where the linear model is too inflexible, we extend the SSGL to sparse generalized additive models by introducing the *nonparametric spike-and-slab lasso* (NPSSL). To our knowledge, our work is the first to apply the spike-and-slab lasso methodology outside of a parametric setting. Our contributions can be summarized as follows:

1. We propose a new group spike-and-slab prior for estimation and variable selection in both parametric and nonparametric settings. Unlike frequentist methods which rely on separable penalties, our model has a *non*-separable and self-adaptive penalty which allows us to automatically adapt to ensemble information about sparsity.
2. We introduce a highly efficient block coordinate ascent algorithm for global posterior mode estimation. This allows us to rapidly identify significant groups of coefficients, while thresholding out insignificant ones.
3. We show that de-biasing techniques that have been used for the original lasso [45] can be extended to our SSGL model to provide valid inference on the estimated regression coefficients.
4. For both grouped regression and sparse additive models, we derive near-optimal posterior contraction rates for both the regression coefficients β and the unknown variance σ^2 under the SSGL prior.

The rest of the paper is structured as follows. In Section 2, we introduce the spike-and-slab group lasso (SSGL). In Section 3, we characterize the global posterior mode and introduce efficient algorithms for fast maximum *a posteriori* (MAP) estimation and variable selection. In Section 4, we utilize ideas from the de-biased lasso to perform inference on the SSGL model. In Section 5, we extend the SSGL to nonparametric settings by proposing

the nonparametric spike-and-slab lasso (NPSSL). In Section 6, we present asymptotic theory for the SSGL and the NPSSL. Finally, in Sections 7 and 8, we provide extensive simulation studies and use our models to analyze real data sets.

1.3 Notation

We use the following notations. For two nonnegative sequences $\{a_n\}$ and $\{b_n\}$, we write $a_n \asymp b_n$ to denote $0 < \liminf_{n \rightarrow \infty} a_n/b_n \leq \limsup_{n \rightarrow \infty} a_n/b_n < \infty$. If $\lim_{n \rightarrow \infty} a_n/b_n = 0$, we write $a_n = o(b_n)$ or $a_n \prec b_n$. We use $a_n \lesssim b_n$ or $a_n = O(b_n)$ to denote that for sufficiently large n , there exists a constant $C > 0$ independent of n such that $a_n \leq Cb_n$. For a vector $\mathbf{v} \in \mathbb{R}^p$, we let $\|\mathbf{v}\|_1 := \sum_{i=1}^p |v_i|$, $\|\mathbf{v}\|_2 := \sqrt{\sum_{i=1}^p v_i^2}$, and $\|\mathbf{v}\|_\infty := \max_{1 \leq i \leq p} |v_i|$ denote the ℓ_1 , ℓ_2 , and ℓ_∞ norms respectively. For a symmetric matrix \mathbf{A} , we let $\lambda_{\min}(\mathbf{A})$ and $\lambda_{\max}(\mathbf{A})$ denote its minimum and maximum eigenvalues.

2 The Spike-and-Slab Group Lasso

Let β_g denote a real-valued vector of length m_g . We define the *group lasso density* as

$$\Psi(\beta_g|\lambda) = C_g \lambda^{m_g} \exp(-\lambda \|\beta_g\|_2), \quad (2.1)$$

where $C_g = 2^{-m_g} \pi^{-(m_g-1)/2} [\Gamma((m_g+1)/2)]^{-1}$. This prior has been previously considered by [19] and [49] for Bayesian inference in the grouped regression model (1.1). Kyung et al. [19] considered a single prior (2.1) on each of the β_g 's, while Xu and Ghosh [49] employed (2.1) as the slab in the point-mass mixture (1.3). These authors implemented their models using MCMC.

In this manuscript, we introduce a *continuous* spike-and-slab prior with the group lasso density (2.1) for both the spike *and* the slab. The continuous nature of our prior is critical in facilitating efficient coordinate ascent algorithms for MAP estimation that allow us to bypass the use of MCMC. Letting $\beta = (\beta_1^T, \dots, \beta_G^T)^T$ under model (1.1), the *spike-and-slab group lasso* (SSGL) is defined as:

$$\pi(\beta|\theta) = \prod_{g=1}^G [(1-\theta)\Psi(\beta_g|\lambda_0) + \theta\Psi(\beta_g|\lambda_1)], \quad (2.2)$$

where $\Psi(\cdot|\lambda)$ denotes the group lasso density (2.1) indexed by hyperparameter λ , and $\theta \in (0, 1)$ is a mixing proportion. λ_0 corresponds to the spike

which shrinks the entire vector β_g towards $\mathbf{0}_{m_g}$, while λ_1 corresponds to the slab. For shorthand notation, we denote $\Psi(\beta_g|\lambda_0)$ as $\Psi_0(\beta_g)$ and $\Psi(\beta_g|\lambda_1)$ as $\Psi_1(\beta_g)$ going forward.

Under the grouped regression model (1.1), we place the SSGL prior (2.2) on β . In accordance with the recommendations of [29], we do not scale our prior by the unknown σ . Instead, we place an independent Jeffreys prior on σ^2 , i.e.

$$\pi(\sigma^2) \propto \sigma^{-2}. \quad (2.3)$$

The mixing proportion θ in (2.2) can either be fixed deterministically or endowed with a prior $\theta \sim \pi(\theta)$. We will discuss this in detail in Section 3.

3 Characterization and Computation of the Global Posterior Mode

Throughout this section, we let p denote the total number of covariates, i.e. $p = \sum_{g=1}^G m_g$. Our goal is to find the maximum *a posteriori* estimates of the regression coefficients $\beta \in \mathbb{R}^p$. This optimization problem is equivalent to a penalized likelihood method in which the logarithm of the prior (2.2) may be reinterpreted as a penalty on the regression coefficients. Similarly to Ročková and George [36], we will leverage this connection between the Bayesian and frequentist paradigms and introduce the SSGL penalty. This strategy combines the adaptivity of the Bayesian approach with the computational efficiency of existing algorithms in the frequentist literature.

A key component of the SSGL model is θ , the prior expected proportion of groups with large coefficients. Ultimately, we will pursue a fully Bayes approach and place a prior on θ , allowing the SSGL to adapt to the underlying sparsity of the data and perform an automatic multiplicity adjustment [38]. For ease of exposition, however, we will first consider the case where θ is fixed, echoing the development of Ročková and George [36]. In this situation, the regression coefficients β_g are conditionally independent *a priori*, resulting in a separable SSGL penalty. Later we will consider the fully Bayes approach, which will yield the *non-separable* SSGL penalty.

Definition 1. Given $\theta \in (0, 1)$, the separable SSGL penalty is defined as

$$\text{pen}_S(\beta|\theta) = \log \left[\frac{\pi(\beta|\theta)}{\pi(\mathbf{0}_p|\theta)} \right] = -\lambda_1 \sum_{g=1}^G \|\beta_g\|_2 + \sum_{g=1}^G \log \left[\frac{p_\theta^*(\mathbf{0}_{m_g})}{p_\theta^*(\beta_g)} \right] \quad (3.1)$$

where

$$p_{\theta}^*(\beta_g) = \frac{\theta \Psi_1(\beta_g)}{\theta \Psi_1(\beta_g) + (1 - \theta) \Psi_0(\beta_g)}. \quad (3.2)$$

The separable SSGL penalty is almost the logarithm of the original prior (2.2); the only modification is an additive constant to ensure that $\text{pen}_S(\mathbf{0}_p|\theta) = 0$. The connection between the SSGL and penalized likelihood methods is made clearer when considering the derivative of the separable SSGL penalty, given in the following lemma.

Lemma 1. *The derivative of the separable SSGL penalty satisfies*

$$\frac{\partial \text{pen}_S(\beta|\theta)}{\partial \|\beta_g\|_2} = -\lambda_{\theta}^*(\beta_g) \quad (3.3)$$

where

$$\lambda_{\theta}^*(\beta_g) = \lambda_1 p_{\theta}^*(\beta_g) + \lambda_0 [1 - p_{\theta}^*(\beta_g)]. \quad (3.4)$$

Similarly to the SSL, the SSGL penalty is a weighted average of the two regularization parameters, λ_1 and λ_0 . The weight $p_{\theta}^*(\beta_g)$ is the conditional probability that β_g was drawn from the slab distribution rather than the spike. Hence, the SSGL features an adaptive regularization parameter which applies different amounts of shrinkage to each group, unlike the group lasso which applies the same shrinkage to each group.

3.1 The Global Posterior Mode

Similarly to the group lasso [53], the separable nature of the penalty (3.1) lends itself naturally to a block coordinate ascent algorithm which cycles through the groups. In this section, we first outline the group updates resulting from the Karush-Kuhn-Tucker (KKT) conditions. The KKT conditions provide necessary conditions for the global posterior mode. We then derive a more refined condition for the global mode to aid in optimization for multimodal posteriors.

Following Huang et al. [15], we assume that within each group, covariates are orthonormal, i.e. $\mathbf{X}_g^T \mathbf{X}_g = n \mathbf{I}_{m_g}$ for $g = 1, \dots, G$. If this assumption does not hold, then the \mathbf{X}_g matrices can be orthonormalized before fitting the model. As noted by Breheny and Huang [4], orthonormalization can be done without loss of generality since the resulting solution can be transformed back to the original scale.

Proposition 1. *The necessary conditions for $\hat{\beta} = (\hat{\beta}_1^T, \dots, \hat{\beta}_G^T)^T$ to be a global mode are:*

$$\mathbf{X}_g^T(\mathbf{Y} - \mathbf{X}\hat{\beta}) = \sigma^2 \lambda_\theta^*(\hat{\beta}_g) \frac{\hat{\beta}_g}{\|\hat{\beta}_g\|_2} \quad \text{for } \hat{\beta}_g \neq \mathbf{0}_{m_g}, \quad (3.5)$$

$$\|\mathbf{X}_g^T(\mathbf{Y} - \mathbf{X}\hat{\beta})\|_2 \leq \sigma^2 \lambda_\theta^*(\hat{\beta}_g) \quad \text{for } \hat{\beta}_g = \mathbf{0}_{m_g}. \quad (3.6)$$

Equivalently,

$$\hat{\beta}_g = \frac{1}{n} \left(1 - \frac{\sigma^2 \lambda_\theta^*(\hat{\beta}_g)}{\|\mathbf{z}_g\|_2} \right)_+ \mathbf{z}_g \quad (3.7)$$

where $\mathbf{z}_g = \mathbf{X}_g^T [\mathbf{Y} - \sum_{l \neq g} \mathbf{X}_l \hat{\beta}_l]$.

Proof. Follows immediately from Lemma 1 and subdifferential Calculus. \square

The above characterization for the global mode is necessary, but not sufficient. A more refined characterization may be obtained by considering the group-wise optimization problem, noting that the global mode is also a maximizer of the g th group, keeping all other groups fixed.

Proposition 2. *The global mode $\hat{\beta}_g = \mathbf{0}_{m_g}$ if and only if $\|\mathbf{z}_g\|_2 \leq \Delta$, where*

$$\Delta = \inf_{\beta_g} \left\{ \frac{n \|\beta_g\|_2}{2} - \frac{\sigma^2 \text{pens}(\beta|\theta)}{\|\beta_g\|_2} \right\}. \quad (3.8)$$

The proof for Proposition 2 can be found in Appendix C. Unfortunately, the threshold Δ is difficult to compute. We instead find an approximation to this threshold. An upper bound is simply that of the soft-threshold solution (3.7), with $\Delta \leq \sigma^2 \lambda^*(\beta_g)$. However, when λ_0 is large, this bound may be improved. Similarly to Ročková and George [36], we provide improved bounds on the threshold in Theorem 1. This result requires the function $h : \mathbb{R}^{m_g} \rightarrow \mathbb{R}$, defined as:

$$h(\beta_g) = [\lambda_\theta^*(\beta_g) - \lambda_1]^2 + \frac{2n}{\sigma^2} \log p_\theta^*(\beta_g).$$

Theorem 1. *When $(\lambda_0 - \lambda_1) > 2\sqrt{n}/\sigma$ and $h(\mathbf{0}_{m_g}) > 0$, the threshold Δ is bounded by:*

$$\Delta^L < \Delta < \Delta^U \quad (3.9)$$

where

$$\Delta^L = \sqrt{2n\sigma^2 \log[1/p_\theta^*(\mathbf{0}_{m_g})]} - \sigma^4 d + \sigma^2 \lambda_1, \quad (3.10)$$

$$\Delta^U = \sqrt{2n\sigma^2 \log[1/p_\theta^*(\mathbf{0}_{m_g})]} + \sigma^2 \lambda_1, \quad (3.11)$$

and

$$0 < d < \frac{2n}{\sigma^2} - \left(\frac{n}{\sigma^2(\lambda_0 - \lambda_1)} - \frac{\sqrt{2n}}{\sigma} \right)^2 \quad (3.12)$$

When λ_0 is large, $d \rightarrow 0$ and the lower bound on the threshold approaches the upper bound, yielding the approximation $\Delta = \Delta^U$. We will ultimately use this approximation in our block coordinate ascent algorithm.

3.2 The Non-Separable SSGL penalty

As discussed earlier, a key reason for adopting a Bayesian strategy is that it allows the model to borrow information across groups and self-adapt to the true underlying sparsity in the data. This is achieved by placing a prior on θ , the proportion of groups with non-zero coefficients. We now outline this fully Bayes strategy and the resulting *non-separable* SSGL penalty. With the inclusion of the prior $\theta \sim \pi(\theta)$, the marginal prior for the regression coefficients has the following form:

$$\pi(\beta) = \int_0^1 \prod_{g=1}^G [\theta \Psi_1(\beta_g) + (1 - \theta) \Psi_0(\beta_g)] d\pi(\theta) \quad (3.13)$$

$$= \left(\prod_{g=1}^G C_g \lambda_1^{m_g} \right) e^{-\lambda_1 \sum_{g=1}^G \|\beta_g\|_2} \int_0^1 \frac{\theta^G}{\prod_{g=1}^G p_\theta^*(\beta_g)} d\pi(\theta), \quad (3.14)$$

The non-separable SSGL penalty is then defined similarly to the separable penalty, where again we have centered the penalty to ensure $\text{pen}_{NS}(\mathbf{0}_p) = 0$.

Definition 2. *The non-separable SSGL (NS-SSGL) penalty with $\theta \sim \pi(\theta)$ is defined as*

$$\text{pen}_{NS}(\beta) = \log \left[\frac{\pi(\beta)}{\pi(\mathbf{0}_p)} \right] = -\lambda_1 \sum_{g=1}^G \|\beta_g\|_2 + \log \left[\frac{\int_0^1 \theta^G / \prod_{g=1}^G p_\theta^*(\beta_g) d\pi(\theta)}{\int_0^1 \theta^G / \prod_{g=1}^G p_\theta^*(\mathbf{0}_{m_g}) d\pi(\theta)} \right]. \quad (3.15)$$

Although the penalty (3.14) appears intractable, intuition is again obtained by considering the derivative. Following the same line of argument as Ročková and George [36], the derivative of (3.14) is given in the following lemma.

Lemma 2.

$$\frac{\partial \text{pen}_{NS}(\beta)}{\partial \|\beta_g\|_2} \equiv \lambda^*(\beta_g; \beta_{\setminus g}), \quad (3.16)$$

where

$$\lambda^*(\beta_g; \beta_{\setminus g}) = p^*(\beta_g; \beta_{\setminus g})\lambda_1 + [1 - p^*(\beta_g; \beta_{\setminus g})]\lambda_0 \quad (3.17)$$

and

$$p^*(\beta_g; \beta_{\setminus g}) \equiv p_{\theta_g}^*(\beta_g), \quad \text{with } \theta_g = \mathbb{E}[\theta | \beta_{\setminus g}]. \quad (3.18)$$

That is, the marginal prior from (3.14) is rendered tractable by considering the each group of regression coefficients separately, conditional on the remaining coefficients. Such a conditional strategy is motivated by the group-wise updates for the separable penalty considered in the previous section. Thus, our optimization strategy for the non-separable penalty will be very similar to the separable case, except instead of a fixed value for θ , we will impute the mean of θ conditioned on the remaining regression coefficients.

We now consider the form of the conditional mean, $\mathbb{E}[\theta | \hat{\beta}_{\setminus g}]$. As noted by Ročková and George [36], when the number of groups is large, this conditional mean can be replaced by $\mathbb{E}[\theta | \hat{\beta}]$; we will proceed with the same approximation. For the prior on θ , we will use the standard beta prior $\theta \sim \mathcal{B}(a, b)$. With the choices $a = 1$ and $b = G$ for these hyperparameters, this prior results in an automatic multiplicity adjustment for the regression coefficients ([38]).

We now examine the conditional distribution $\pi(\theta | \hat{\beta})$. Suppose that the number of groups with non-zero coefficients is \hat{q} , and assume without loss of generality that the first \hat{q} groups have non-zero coefficients. Then,

$$\pi(\theta | \hat{\beta}) \propto \theta^{a-1} (1 - \theta)^{b-1} (1 - \theta z)^{G-\hat{q}} \prod_{g=1}^{\hat{q}} (1 - \theta x_g), \quad (3.19)$$

with $z = 1 - \frac{\lambda_1}{\lambda_0}$ and $x_g = (1 - \frac{\lambda_1}{\lambda_0} e^{\|\hat{\beta}_g\|_2(\lambda_0 - \lambda_1)})$. Similarly to Ročková and George [36], this distribution is a generalization of the Gauss hypergeometric

distribution. Consequently, the expectation may be written as

$$\mathbb{E}[\theta|\hat{\beta}] = \frac{\int_0^1 \theta^a (1-\theta)^{b-1} (1-\theta z)^{G-\hat{q}} \prod_{g=1}^{\hat{q}} (1-\theta x_g) d\theta}{\int_0^1 \theta^{a-1} (1-\theta)^{b-1} (1-\theta z)^{G-\hat{q}} \prod_{g=1}^{\hat{q}} (1-\theta x_g) d\theta}. \quad (3.20)$$

While the above expression (3.20) appears laborious to compute, it admits a much simpler form when λ_0 is very large. Using a slight modification to the arguments of [33], we obtain this simpler form in Lemma 3.

Lemma 3. *Assume $\pi(\theta|\hat{\beta})$ is distributed according to (3.19). Let \hat{q} be the number of groups with non-zero coefficients. Then as $\lambda_0 \rightarrow \infty$,*

$$\mathbb{E}[\theta|\hat{\beta}] = \frac{a + \hat{q}}{a + b + G}. \quad (3.21)$$

The proof for Lemma 3 is in Appendix C. We note that the expression (3.21) is essentially the usual posterior mean of θ under a beta prior. Intuitively, as λ_0 diverges, the weights $p_{\theta}^*(\beta_g)$ concentrate at zero and one, yielding the familiar form for $\mathbb{E}[\theta|\hat{\beta}]$. With this in hand, we are now in a position to outline the block coordinate ascent algorithm for the non-separable SSGL.

3.3 Optimization

The KKT conditions for the non-separable SSGL penalty yield the following necessary condition for the global mode:

$$\hat{\beta}_g \leftarrow \frac{1}{n} \left(1 - \frac{\sigma^2 \lambda_{\hat{\theta}}^*(\hat{\beta}_g)}{\|z_g\|_2} \right)_+ z_g, \quad (3.22)$$

where $z_g = \mathbf{X}_g^T [\mathbf{Y} - \sum_{l \neq g} \mathbf{X}_l \hat{\beta}_l]$ and $\hat{\theta}$ is the mean (3.21), conditioned on the previous value of β . As before, (3.22) is sufficient for a local mode, but not the global mode. When $p \gg n$ and λ_0 is large, the posterior will be highly multimodal. As in the separable case, we require a refined thresholding scheme that will eliminate some of these suboptimal local modes from consideration. In approximating the group-wise conditional mean $\mathbb{E}[\theta|\hat{\beta}_{\setminus g}]$ with $\mathbb{E}[\theta|\hat{\beta}]$, we do not require group-specific thresholds. Instead, we can use the threshold given in Proposition 2 and Theorem 1 where θ is replaced with the current update (3.21). In particular, we shall use the upper bound Δ^U in our block coordinate ascent algorithm.

Similarly to Ročková and George [36], we combine the refined threshold, Δ^U with the soft thresholding operation (3.22), to yield the following update for $\hat{\beta}_g$ at iteration k :

$$\beta_g^{(k)} \leftarrow \frac{1}{n} \left(1 - \frac{\sigma^{2(k)} \lambda^*(\beta_g^{(k-1)}; \theta^{(k)})}{\|z_g\|_2} \right)_+ z_g \mathbb{I}(\|z_g\|_2 > \Delta^U) \quad (3.23)$$

where $\theta^{(k)} = \mathbb{E}[\theta | \beta^{(k-1)}]$. Technically, θ should be updated after each group β_g is updated. In practice, however, there will be little change after one group is updated and so we will update both θ and Δ^U after every M iterations with a default value of $M = 10$.

With the Jeffreys prior $\pi(\sigma^2) \propto \sigma^{-2}$, the error variance σ^2 also has a closed form update:

$$\sigma^{2(k)} \leftarrow \frac{\|\mathbf{Y} - \mathbf{X}\beta^{(k-1)}\|_2^2}{n + 2}. \quad (3.24)$$

The complete optimization algorithm is given in Algorithm 1. The computational complexity of Algorithm 1 is $\mathcal{O}(np)$ per iteration, where $p = \sum_{g=1}^G m_g$. It takes $\mathcal{O}(nm_g)$ operations to compute the partial residual z_g for the g th group, for a total cost of $\mathcal{O}(n \sum_{g=1}^G m_g) = \mathcal{O}(np)$. Similarly, it takes $\mathcal{O}(np)$ cost to compute the sum of squared residuals $\|\mathbf{Y} - \mathbf{X}\hat{\beta}\|_2^2$ to update the variance parameter σ^2 . The computational complexity of our algorithm matches that of the usual gradient descent algorithms for lasso and group lasso [10].

As a non-convex method, it is not guaranteed that SSGL will find the global posterior mode, only a local mode. However, the refined thresholding scheme (Theorem 1) and a warm start initialization strategy (described in detail in Appendix A) enable SSGL to eliminate a number sub-optimal local modes from consideration in a similar manner to Ročková and George [36]. To briefly summarize the initialization strategy, we tune λ_0 from an increasing sequence of values, and we further scale λ_0 by $\sqrt{m_g}$ for each g th group to ensure that the amount of penalization is on the same scale for groups of potentially different sizes [53]. Meanwhile, we keep λ_1 fixed at a small value so that selected groups have minimal shrinkage. See Appendix A for detailed discussion of choosing (λ_0, λ_1) .

4 Approaches to Inference

While the above procedure allows us to find the posterior mode of β , providing a measure of uncertainty around our estimate is a challenging task.

Algorithm 1 Spike-and-Slab Group Lasso

Input: grid of increasing λ_0 values $I = \{\lambda_0^1, \dots, \lambda_0^L\}$, update frequency M

For $l = 1, \dots, L$:

1. Set iteration counter $k_l = 0$
2. Initialize: $\hat{\beta}^{(k_l)} = \beta^*$, $\theta^{(k_l)} = \theta^*$, $\sigma^{(k_l)2} = \sigma^{*2}$, $\Delta^U = \Delta^*$
3. While $\text{diff} > \varepsilon$
 - (a) Increment k_l
 - (b) For $g = 1, \dots, G$:
 - i. Update

$$\beta_g^{(k_l)} \leftarrow \frac{1}{n} \left(1 - \frac{\sigma^{(k_l)2} \lambda^*(\beta_g^{(k_l-1)}; \theta^{(k_l)})}{\|\mathbf{z}_g\|_2} \right)_+ \mathbf{z}_g \mathbb{I}(\|\mathbf{z}_g\|_2 > \Delta^U)$$

- ii. Update

$$\hat{Z}_g = \begin{cases} 1 & \text{if } \beta_g^{(k_l)} \neq \mathbf{0}_{m_g} \\ 0 & \text{otherwise} \end{cases}$$

- iii. If $g \equiv 0 \pmod{M}$:

- A. Update

$$\theta^{(k_l)} \leftarrow \frac{a + \sum_{g=1}^G \hat{Z}_g}{a + b + G}$$

- B. If $k_{l-1} < 100$:

$$\text{Update } \sigma^{(k_l)2} \leftarrow \frac{\|\mathbf{Y} - \mathbf{X}\beta^{(k_l)}\|_2^2}{n + 2}$$

- C. Update

$$\Delta^U \leftarrow \begin{cases} \sqrt{2n\sigma^{(k_l)2} \log[1/p^*(\mathbf{0}_{m_g}; \theta^{(k_l)})]} + \sigma^{(k_l)2} \lambda_1 & \text{if } h(\mathbf{0}_{m_g}; \theta^{(k_l)}) > 0 \\ \sigma^{(k_l)2} \lambda^*(\mathbf{0}_{m_g}; \theta^{(k_l)}) & \text{otherwise} \end{cases}$$

- iv. $\text{diff} = \|\beta^{(k_l)} - \beta^{(k_l-1)}\|_2$
-

One possible solution is to run MCMC where the algorithm is initialized at the posterior mode. By starting the MCMC chain at the mode, the algorithm should converge faster. However, this is still not ideal, as it can be computationally burdensome in high dimensions. Instead, we will adopt ideas from a recent line of research [46, 17] based on de-biasing estimates from high-dimensional regression. These ideas were derived in the context of lasso regression, and we will explore the extent to which they work for the SSGL penalty. Define $\hat{\Sigma} = \mathbf{X}^T \mathbf{X} / n$ and let $\hat{\Theta}$ be an approximate inverse

of $\widehat{\Sigma}$. We define

$$\widehat{\beta}_d = \widehat{\beta} + \widehat{\Theta} \mathbf{X}^T (\mathbf{Y} - \mathbf{X} \widehat{\beta}) / n. \quad (4.1)$$

where $\widehat{\beta}$ is the MAP estimator of β under the SSGL model. By [46], this quantity $\widehat{\beta}_d$ has the following asymptotic distribution:

$$\sqrt{n}(\widehat{\beta}_d - \beta) \sim \mathcal{N}(\mathbf{0}, \sigma^2 \widehat{\Theta} \widehat{\Sigma} \widehat{\Theta}^T). \quad (4.2)$$

For our inference procedure, we replace the population variance σ^2 in (4.2) with the modal estimate $\widehat{\sigma}^2$ from the SSGL model. To estimate $\widehat{\Theta}$, we utilize the nodewise regression approach described in [25, 46]. We describe this estimation procedure for $\widehat{\Theta}$ in Appendix A.

Let $\widehat{\beta}_{dj}$ denote the j th coordinate of $\widehat{\beta}_d$. We have from (4.2) that the $100(1 - \alpha)\%$ asymptotic pointwise confidence intervals for $\beta_j, j = 1, \dots, p$, are

$$[\widehat{\beta}_{dj} - c(\alpha, n, \widehat{\sigma}^2), \widehat{\beta}_{dj} + c(\alpha, n, \widehat{\sigma}^2)], \quad (4.3)$$

where $c(\alpha, n, \widehat{\sigma}^2) := \Phi^{-1}(1 - \alpha/2) \sqrt{\widehat{\sigma}^2 (\widehat{\Theta} \widehat{\Sigma} \widehat{\Theta}^T)_{jj} / n}$ and $\Phi(\cdot)$ denotes the cumulative distribution function of $\mathcal{N}(0, 1)$. It should be noted that our posterior mode estimates should have less bias than existing estimates such as the group lasso. Therefore, the goal of the de-biasing procedure is less about de-biasing the posterior mode estimates, and more about providing an estimator with an asymptotic normal distribution from which we can perform inference.

To assess the ability of this procedure to obtain accurate confidence intervals (4.3) with $\alpha = 0.05$, we run a small simulation study with $n = 100$, $G = 100$ or $n = 300, G = 300$, and each of the G groups having $m = 2$ covariates. We generate the covariates from a multivariate normal distribution with mean $\mathbf{0}$ and an AR(1) covariance structure with correlation ρ . The two covariates from each group are the linear and squared term from the original covariates. We set the first seven elements of β equal to $(0, 0.5, 0.25, 0.1, 0, 0, 0.7)$ and the remaining elements equal to zero. Lastly, we try $\rho = 0$ and $\rho = 0.7$. Table 1 shows the coverage probabilities across 1000 simulations for all scenarios looked at. We see that important covariates, i.e. covariates with a nonzero corresponding β_j , have coverage near 0.85 when $n = 100$ under either correlation structure, though this increases to nearly the nominal rate when $n = 300$. The remaining covariates (null covariates) achieve the nominal level regardless of the sample size or correlation present.

| | ρ | Important covariates | Null covariates |
|--------------------|--------|----------------------|-----------------|
| $n = 100, G = 100$ | 0.0 | 0.83 | 0.93 |
| | 0.7 | 0.85 | 0.94 |
| $n = 300, G = 300$ | 0.0 | 0.93 | 0.95 |
| | 0.7 | 0.92 | 0.95 |

Table 1: Coverage probabilities for de-biasing simulation.

5 Nonparametric Spike-and-Slab Lasso

We now introduce the nonparametric spike-and-slab lasso (NPSSL). The NPSSL allows for flexible modeling of a response surface with minimal assumptions regarding its functional form. We consider two cases for the NPSSL: (i) a main effects only model, and (ii) a model with both main and interaction effects.

5.1 Main Effects

We first consider the main effects NPSSL model. Here, we assume that the response surface may be decomposed into the sum of univariate functions of each of the p covariates. That is, we have the following model:

$$y_i = \sum_{j=1}^p f_j(X_{ij}) + \varepsilon_i, \quad \varepsilon_i \sim \mathcal{N}(0, \sigma^2). \quad (5.1)$$

Following Ravikumar et al. [32], we assume that each f_j , $j = 1, \dots, p$, may be approximated by a linear combination of basis functions $\mathcal{B}_j = \{g_{j1}, \dots, g_{jd}\}$, i.e.,

$$f_j(X_{ij}) \approx \sum_{k=1}^d g_{jk}(X_{ij})\beta_{jk} \quad (5.2)$$

where $\beta_j = (\beta_{j1}, \dots, \beta_{jd})^T$ are the unknown weights. Let $\widetilde{\mathbf{X}}_j$ denote the $n \times d$ matrix with the (i, k) th entry $\widetilde{\mathbf{X}}_j(i, k) = g_{jk}(X_{ij})$. Then, (5.1) may be represented in matrix form as

$$\mathbf{Y} - \boldsymbol{\delta} = \sum_{j=1}^p \widetilde{\mathbf{X}}_j \beta_j + \boldsymbol{\varepsilon}, \quad \boldsymbol{\varepsilon} \sim \mathcal{N}_n(\mathbf{0}, \sigma^2 \mathbf{I}_n), \quad (5.3)$$

where $\boldsymbol{\delta}$ is a vector of the lower-order truncation bias. Note that we assume the response \mathbf{Y} has been centered and so we do not include a grand mean

μ in (5.3). Thus, we do not require the main effects to integrate to zero as in Wei et al. [48]. We do, however, require the matrices $\widetilde{\mathbf{X}}_j, j = 1, \dots, p$, to be orthogonal, as discussed in Section 3. Note that the entire design matrix does not need to be orthogonal; only the group-specific matrices need to be. We can enforce this in practice by either using orthonormal basis functions or by orthonormalizing the $\widetilde{\mathbf{X}}_j$ matrices before fitting the model.

We assume that \mathbf{Y} depends on only a small number of the p covariates so that many of the f_j 's have a negligible contribution to (5.1). This is equivalent to assuming that most of the weight vectors β_j have all zero elements. If the j th covariate is determined to be predictive of \mathbf{Y} , then f_j has a non-negligible contribution to (5.1). In this case, we want to include the *entire* basis function approximation to f_j in the model.

The above situation is a natural fit for the SSGL. We have p groups where each group is either included as a whole or not included in the model. The design matrices for each group are exactly the matrices of basis functions, $\widetilde{\mathbf{X}}_j, j = 1, \dots, p$. We will utilize the non-separable SSGL penalty developed in Section 3.2 to enforce this group-sparsity behavior in the model (5.3). More specifically, we seek to maximize the objective function with respect to $\beta = (\beta_1^T, \dots, \beta_p^T)^T \in \mathbb{R}^{pd}$ and σ^2 :

$$L(\beta, \sigma^2) = -\frac{1}{2\sigma^2} \|\mathbf{Y} - \sum_{j=1}^p \widetilde{\mathbf{X}}_j \beta_j\|_2^2 - (n+2) \log \sigma + \text{pen}_{NS}(\beta). \quad (5.4)$$

To find the estimators of β and σ^2 , we use Algorithm 1. Similar additive models have been proposed by a number of authors including Ravikumar et al. [32] and Wei et al. [48]. However, our proposed NPSSL method has a number of advantages. First, we allow the noise variance σ^2 to be unknown, unlike Ravikumar et al. [32]. Accurate estimates of σ^2 are important to avoid overfitting the noise beyond the signal. Secondly, we use a block-descent algorithm to quickly target the modes of the posterior, whereas Wei et al. [48] utilize MCMC. Finally, our SSGL algorithm automatically thresholds negligible groups to zero, negating the need for a post-processing thresholding step.

5.2 Main and Interaction Effects

The main effects model (5.1) allows for each covariate to have a nonlinear contribution to the model, but assumes a linear relationship *between* the covariates. In some applications, this assumption may be too restrictive. For example, in the environmental exposures data which we analyze in Section

8.2, we may expect high levels of two toxins to have an even more adverse effect on a person's health than high levels of either of the two toxins. Such an effect may be modeled by including interaction effects between the covariates.

Here, we extend the NPSSL to include interaction effects. We consider only second-order interactions between the covariates, but our model can easily be extended to include even higher-order interactions. We assume that the interaction effects may be decomposed into the sum of bivariate functions of each pair of covariates, yielding the model:

$$y_i = \sum_{j=1}^p f_j(X_{ij}) + \sum_{k=1}^{p-1} \sum_{l=k+1}^p f_{kl}(X_{ik}, X_{il}) + \varepsilon_i, \quad \varepsilon_i \sim \mathcal{N}(0, \sigma^2). \quad (5.5)$$

For the interaction terms, we follow Wei et al. [48] and approximate f_{kl} using the outer product of the basis functions of the interacting covariates:

$$f_{kl}(X_{ik}, X_{il}) \approx \sum_{s=1}^{d^*} \sum_{r=1}^{d^*} g_{ks}(X_{ik}) g_{lr}(X_{il}) \beta_{kl sr} \quad (5.6)$$

where $\beta_{kl} = (\beta_{kl11}, \dots, \beta_{kl1d^*}, \beta_{kl21}, \dots, \beta_{kl d^* d^*})^T \in \mathbb{R}^{d^{*2}}$ is the vector of unknown weights. We let \mathbf{X}_{kl} denote the $n \times d^{*2}$ matrix with rows

$$\widetilde{\mathbf{X}}_{kl}(i, \cdot) = \text{vec}(\mathbf{g}_k(X_{ik}) \mathbf{g}_l(X_{il})^T),$$

where $\mathbf{g}_k(X_{ik}) = (g_{k1}(X_{ik}), \dots, g_{kd^*}(X_{ik}))^T$. Then, (5.5) may be represented in matrix form as

$$\mathbf{Y} - \boldsymbol{\delta} = \sum_{j=1}^p \widetilde{\mathbf{X}}_j \boldsymbol{\beta}_j + \sum_{k=1}^{p-1} \sum_{l=k+1}^p \widetilde{\mathbf{X}}_{kl} \boldsymbol{\beta}_{kl} + \boldsymbol{\varepsilon}, \quad \boldsymbol{\varepsilon} \sim \mathcal{N}_n(\mathbf{0}, \sigma^2 \mathbf{I}_n), \quad (5.7)$$

where $\boldsymbol{\delta}$ is a vector of the lower-order truncation bias. We again assume \mathbf{Y} has been centered and so do not include a grand mean in (5.7). We do not constrain f_{kl} to integrate to zero as in Wei et al. [48]. However, we do ensure that the main effects are not in the linear span of the interaction functions. That is, we require the “main effect” matrices $\widetilde{\mathbf{X}}_l$ and $\widetilde{\mathbf{X}}_k$ to be orthogonal to the “interaction” matrix $\widetilde{\mathbf{X}}_{kl}$. This condition is needed to maintain identifiability for both the main and interaction effects in the model. In practice, we enforce this condition by setting the interaction design matrix to be the residuals of the regression of $\widetilde{\mathbf{X}}_k \circ \widetilde{\mathbf{X}}_l$ on $\widetilde{\mathbf{X}}_k$ and $\widetilde{\mathbf{X}}_l$.

Note that the current representation does not enforce strong hierarchy. That is, interaction terms can be included even if their corresponding main effects are removed from the model. However, the NPSSL model can be easily modified to accommodate strong hierarchy. If hierarchy is desired, the “interaction” matrices can be augmented to contain both main and interaction effects, as in [22], i.e. the “interaction” matrices in (5.7) would be $\widetilde{\mathbf{X}}_{kl}^{\text{aug}} = [\widetilde{\mathbf{X}}_k, \widetilde{\mathbf{X}}_l, \widetilde{\mathbf{X}}_{kl}]$, instead of simply $\widetilde{\mathbf{X}}_{kl}$. This augmented model is overparameterized since the main effects still have their own separate design matrices as well (to ensure that main effects can still be selected even if $\beta_{kl}^{\text{aug}} = \mathbf{0}$). However, this ensures that interaction effects are only selected if the corresponding main effects are also in the model.

In the interaction model, we either include β_{kl} in the model (5.7) if there is a non-negligible interaction between the k th and l th covariates, or we estimate $\hat{\beta}_{kl} = \mathbf{0}_{d^*2}$ if such an interaction is negligible. With the non-separable SSSL penalty, the objective function is:

$$L(\beta, \sigma^2) = -\frac{1}{2\sigma^2} \|\mathbf{Y} - \sum_{j=1}^p \widetilde{\mathbf{X}}_j \beta_j - \sum_{k=1}^{p-1} \sum_{l=k+1}^p \widetilde{\mathbf{X}}_{kl} \beta_{kl}\|_2^2 + \text{pen}_{NS}(\beta) - (n+2) \log \sigma, \quad (5.8)$$

where $\beta = (\beta_1^T, \dots, \beta_p^T, \beta_{12}^T, \dots, \beta_{(p-1)p}^T)^T \in \mathbb{R}^{pd+p(p-1)d^*2/2}$. We can again use Algorithm 1 to find the modal estimates of β and σ^2 .

6 Asymptotic Theory for the SSSL and NPSSL

In this section, we derive asymptotic properties for the separable SSSL and NPSSL models. We first note some differences between our theory and the theory in Ročková and George [36]. First, we prove *joint* consistency in estimation of both the unknown β and the unknown σ^2 , whereas [36] proved their result only for β , assuming known variance $\sigma^2 = 1$. Secondly, Ročková and George [36] established posterior contraction rates for the global posterior mode and the full posterior separately, whereas we establish a contraction rate ϵ_n for the full posterior only. Our rate ϵ_n satisfies $\epsilon_n \rightarrow 0$ as $n \rightarrow \infty$ (i.e. the full posterior collapses to the true (β, σ^2) almost surely as $n \rightarrow \infty$), and hence, it automatically follows that the posterior mode is a consistent estimator of (β, σ^2) . Finally, we also derive a posterior contraction rate for nonparametric additive regression, not just linear regression. All proofs for the theorems in this section can be found in Appendix C.

6.1 Grouped Linear Regression

We work under the frequentist assumption that there is a true model,

$$\mathbf{Y} = \sum_{g=1}^G \mathbf{X}_g \beta_{0g} + \varepsilon, \quad \varepsilon \sim \mathcal{N}_n(\mathbf{0}, \sigma_0^2 \mathbf{I}_n), \quad (6.1)$$

where $\beta_0 = (\beta_{01}^T, \dots, \beta_{0G}^T)^T$ and $\sigma_0^2 \in (0, \infty)$. Denote $\mathbf{X} = [\mathbf{X}_1, \dots, \mathbf{X}_G]$ and $\beta = (\beta_1^T, \dots, \beta_G^T)^T$. Suppose we endow (β, σ^2) under model (6.1) with the prior specification:

$$\begin{aligned} \pi(\beta|\theta) &\sim \prod_{g=1}^G [(1-\theta)\Psi(\beta_g|\lambda_0) + \theta\Psi(\beta_g|\lambda_1)], \\ \sigma^2 &\sim \mathcal{IG}(c_0, d_0), \end{aligned} \quad (6.2)$$

where $c_0 > 0$ and $d_0 > 0$ are fixed constants and θ is set deterministically.

Remark 1. In our implementation of the SSGL model, we endowed σ^2 with an improper prior, $\pi(\sigma^2) \propto \sigma^{-2}$. This can be viewed as a limiting case of the $\mathcal{IG}(c_0, d_0)$ prior with $c_0 \rightarrow 0, d_0 \rightarrow 0$. This improper prior is fine for implementation since it leads to a proper posterior, but for our theoretical investigation, we require the priors on (β, σ^2) to be proper.

6.1.1 Posterior Contraction Rates

Let $m_{\max} = \max_{1 \leq j \leq G} m_j$ and let $p = \sum_{g=1}^G m_g$. Let S_0 be the set containing the indices of the true nonzero groups, where $S_0 \subseteq \{1, \dots, G\}$ with cardinality $s_0 = |S_0|$. We make the following assumptions:

- (A1) Assume that $G \gg n$, $\log(G) = o(n)$, and $m_{\max} = O(\log G / \log n)$.
- (A2) The true number of nonzero groups satisfies $s_0 = o(n / \log G)$.
- (A3) There exists a constant $k > 0$ so that $\lambda_{\max}(\mathbf{X}^T \mathbf{X}) \leq kn^\alpha$, for some $\alpha \in [1, \infty)$.
- (A4) Let $\xi \subset \{1, \dots, G\}$, and let \mathbf{X}_ξ denote the submatrix of \mathbf{X} that contains the submatrices with groups indexed by ξ . There exist constants $\nu_1 > 0$, $\nu_2 > 0$, and an integer \bar{p} satisfying $s_0 = o(\bar{p})$ and $\bar{p} = o(s_0 \log n)$, so that $n\nu_1 \leq \lambda_{\min}(\mathbf{X}_\xi^T \mathbf{X}_\xi) \leq \lambda_{\max}(\mathbf{X}_\xi^T \mathbf{X}_\xi) \leq n\nu_2$ for any model of size $|\xi| \leq \bar{p}$.
- (A5) $\|\beta_0\|_\infty = O(\log G)$.

Assumption (A1) allows the number of groups G and total number of covariates p to grow at nearly exponential rate with sample size n . The size of each individual group may also grow as n grows, but should grow at a slower rate than $n/\log n$. Assumption (A2) specifies the growth rate for the true model size s_0 . Assumption (A3) bounds the eigenvalues of $\mathbf{X}^T \mathbf{X}$ from above and is less stringent than requiring all the eigenvalues of the Gram matrix $(\mathbf{X}^T \mathbf{X}/n)$ to be bounded away from infinity. Assumption (A4) ensures that $\mathbf{X}^T \mathbf{X}$ is locally invertible over sparse sets. In general, conditions (A3)-(A4) are difficult to verify, but they can be shown to hold with high probability for certain classes of matrices where the rows of \mathbf{X} are independent and sub-Gaussian [26, 31]. Finally, Assumption (A5) places a restriction on the growth rate of the maximum signal size for the true β_0 .

We now state our main theorem on the posterior contraction rates for the SSGL prior (6.2) under model (6.1). Let \mathbb{P}_0 denote the probability measure underlying the truth (6.1) and $\Pi(\cdot|\mathbf{Y})$ denote the posterior distribution under the prior specification (6.2) for (β, σ^2) .

Theorem 2 (posterior contraction rates). *Let $\epsilon_n = \sqrt{s_0 \log G/n}$, and suppose that Assumptions (A1)-(A5) hold. Under model (6.1), suppose we endow (β, σ^2) with the prior (6.2). Further assume that $\lambda_0 = (1 - \theta)/\theta = G^c$ where $c \geq 2$, and $\lambda_1 \asymp 1/n$. Then*

$$\Pi(\beta : \|\beta - \beta_0\|_2 \geq M_1 \sigma_0 \epsilon_n | \mathbf{Y}) \rightarrow 0 \text{ a.s. } \mathbb{P}_0 \text{ as } n, G \rightarrow \infty \quad (6.3)$$

$$\Pi(\beta : \|\mathbf{X}\beta - \mathbf{X}\beta_0\|_2 \geq M_2 \sigma_0 \sqrt{n} \epsilon_n | \mathbf{Y}) \rightarrow 0 \text{ a.s. } \mathbb{P}_0 \text{ as } n, G \rightarrow \infty, \quad (6.4)$$

$$\Pi(\sigma^2 : |\sigma^2 - \sigma_0^2| \geq 4\sigma_0^2 \epsilon_n | \mathbf{Y}) \rightarrow 0 \text{ as } n \rightarrow \infty, \text{ a.s. } \mathbb{P}_0 \text{ as } n, G \rightarrow \infty, \quad (6.5)$$

for some $M_1 > 0, M_2 > 0$.

Remark 2. *In the case where $G = p$ and $m_1 = \dots = m_G = 1$, the ℓ_2 and prediction error rates in (6.3)-(6.4) reduce to the familiar optimal rates of $\sqrt{s_0 \log p/n}$ and $\sqrt{s_0 \log p}$ respectively.*

Remark 3. *Eq. (6.5) demonstrates that our model also consistently estimates the unknown variance σ^2 , therefore providing further theoretical justification for placing an independent prior on σ^2 , as advocated by Moran et al. [29].*

6.1.2 Dimensionality Recovery

Although the posterior mode is exactly sparse, the SSGL prior is absolutely continuous so it assigns zero mass to exactly sparse vectors. To approximate

the model size under the SSGL model, we use the following generalized notion of sparsity [3]. For $\omega_g > 0$, we define the generalized inclusion indicator and generalized dimensionality, respectively, as

$$\gamma_{\omega_g}(\beta_g) = I(\|\beta_g\|_2 > \omega_g) \text{ and } |\gamma(\beta)| = \sum_{g=1}^G \gamma_{\omega_g}(\beta_g). \quad (6.6)$$

In contrast to [3, 36], we allow the threshold ω_g to be different for each group, owing to the fact that the group sizes m_g may not necessarily all be the same. However, the ω_g 's, $g = 1, \dots, G$, should still tend towards zero as n increases, so that $|\gamma(\beta)|$ provides a good approximation to $\#\{g : \beta_g \neq \mathbf{0}_{m_g}\}$.

Consider as the threshold,

$$\omega_g \equiv \omega_g(\lambda_0, \lambda_1, \theta) = \frac{1}{\lambda_0 - \lambda_1} \log \left[\frac{1 - \theta}{\theta} \frac{\lambda_0^{m_g}}{\lambda_1^{m_g}} \right] \quad (6.7)$$

Note that for large λ_0 , this threshold rapidly approaches zero. Analogous to [34] and [36], any vectors β_g that satisfy $\|\beta_g\|_2 = \omega_g$ correspond to the intersection points between the two group lasso densities in the separable SSGL prior (2.2), or when the second derivative $\partial^2 \text{pen}_S(\beta|\theta)/\partial \|\beta_g\|_2^2 = 0.5$. The value ω_g represents the turning point where the slab has dominated the spike, and thus, the sharper the spike (when λ_0 is large), the smaller the threshold.

Using the notion of generalized dimensionality (6.6) with (6.7) as the threshold, we have the following theorem.

Theorem 3 (dimensionality). *Suppose that Assumptions (A1)-(A5) hold. Further assume that $\lambda_0 = (1 - \theta)/\theta = G^c$ where $c \geq 2$, and $\lambda_1 \asymp 1/n$. Then for sufficiently large $M_3 > 0$,*

$$\sup_{\beta_0} \mathbb{E}_{\beta_0} \Pi(\beta : |\gamma(\beta)| > M_3 s_0 | \mathbf{Y}) \rightarrow 0 \text{ as } n, G \rightarrow \infty. \quad (6.8)$$

Theorem 3 shows that the expected posterior probability that the generalized dimension is a constant multiple larger than the true model size s_0 is asymptotically vanishing. In other words, the SSGL posterior concentrates on sparse sets.

6.2 Sparse Generalized Additive Models (GAMs)

We also derive contraction rates for the NPSSL model. Assume there is a true model,

$$y_i = \sum_{j=1}^p f_{0j}(X_{ij}) + \varepsilon_i, \quad \varepsilon_i \sim \mathcal{N}(0, \sigma_0^2) \quad (6.9)$$

where $f_{0j}, j = 1, \dots, p$, denotes the true unknown smooth function and $\sigma_0^2 \in (0, \infty)$. Suppose each f_{0j} can be approximated by a linear combination of basis functions, $\{g_{j1}, \dots, g_{jd}\}$. In matrix notation, (6.9) can be written as

$$\mathbf{Y} = \sum_{j=1}^p \widetilde{\mathbf{X}}_j \boldsymbol{\beta}_{0j} + \boldsymbol{\delta} + \boldsymbol{\varepsilon}, \quad \boldsymbol{\varepsilon} \sim \mathcal{N}_n(\mathbf{0}, \sigma_0^2 \mathbf{I}_n), \quad (6.10)$$

where $\widetilde{\mathbf{X}}_j$ denotes an $n \times d$ matrix where the (i, k) th entry is $\widetilde{\mathbf{X}}_j(i, k) = g_{jk}(X_{ij})$, $\boldsymbol{\beta}_{0j}$'s are $d \times 1$ vectors of basis coefficients, and $\boldsymbol{\delta}$ denotes an $n \times 1$ vector of lower-order bias.

Denote $\widetilde{\mathbf{X}} = [\widetilde{\mathbf{X}}_1, \dots, \widetilde{\mathbf{X}}_p]$ and $\boldsymbol{\beta} = (\boldsymbol{\beta}_1^T, \dots, \boldsymbol{\beta}_p^T)^T$. Under (6.9), suppose we endow $(\boldsymbol{\beta}, \sigma^2)$ in (6.10) with the prior specification (6.2). We have the following assumptions:

- (B1) Suppose that $p \gg n$ and $d \rightarrow \infty$ as $n \rightarrow \infty$, but that $\log p = o(n)$ and $d = O(\log p / \log n)$.
- (B2) The true number of nonzero functions satisfies $s_0 = o(n / \log p)$.
- (B3) There exists a constant $k_1 > 0$ so that for all n , $\lambda_{\max}(\widetilde{\mathbf{X}}^T \widetilde{\mathbf{X}}) \leq k_1 n$.
- (B4) Let $\xi \subset \{1, \dots, p\}$, and let $\widetilde{\mathbf{X}}_\xi$ denote the submatrix of $\widetilde{\mathbf{X}}$ that contains the submatrices indexed by ξ . There exists a constant $\nu_1 > 0$ and an integer \bar{p} satisfying $s_0 = o(\bar{p})$ and $\bar{p} = o(s_0 \log n)$, so that $\lambda_{\min}(\widetilde{\mathbf{X}}_\xi^T \widetilde{\mathbf{X}}_\xi) \geq n\nu_1$ for any model of size $|\xi| \leq \bar{p}$.
- (B5) $\|\boldsymbol{\beta}_0\|_\infty = O(\log p)$.
- (B6) All the functions $f_{0j}, j = 1, \dots, p$, are κ -times continuously differentiable for some $\kappa > 0$, so that the bias $\boldsymbol{\delta}$ satisfies $\|\boldsymbol{\delta}\|_\infty \lesssim d^{-\kappa}$.

Assumptions (B1)-(B5) are analogous to assumptions (A1)-(A5). Assumptions (B3)-(B4) are difficult to verify but can be shown to hold if the covariates are uniformly bounded and appropriate basis functions for the g_{jk} 's are used, e.g. cubic B-splines [52, 48]. Finally, Assumption (B6) defines the minimum smoothness for all additive functions, so that the bias incurred by a d -dimensional basis expansion is asymptotically on the order of $d^{-\kappa}$. Assumption (B6) is satisfied, for example, by spline basis functions [8].

Let $\tilde{\mathbb{P}}_0$ denote the probability measure underlying the truth (6.9) and $\Pi(\cdot | \mathbf{Y})$ denote the posterior distribution under NPSSL model with the prior (6.2) for $(\boldsymbol{\beta}, \sigma^2)$ in (6.10). Further, let $f(\mathbf{X}_i) = \sum_{j=1}^p f_j(X_{ij})$ and $f_0(\mathbf{X}_i) =$

$\sum_{j=1}^p f_{0j}(X_{ij})$, and define the empirical norm $\|\cdot\|_n$ as

$$\|f - f_0\|_n^2 = \frac{1}{n} \sum_{i=1}^n [f(\mathbf{X}_i) - f_0(\mathbf{X}_i)]^2.$$

Let \mathcal{F} denote the infinite-dimensional set of all possible additive functions f_0 . The next theorem establishes the posterior contraction rate under the NPSSL model.

Theorem 4 (contraction rates). *Let $\epsilon_n = \max\{\sqrt{s_0 \log p/n}, d^{-\kappa}\}$. Suppose that Assumptions (B1)-(B6) hold. Suppose we endow (β, σ^2) under model (6.10) with the prior (6.2). Further assume that $\lambda_0 = (1 - \theta)/\theta = p^c$ where $c \geq 2$, and $\lambda_1 \asymp 1/n$. Then*

$$\Pi\left(f \in \mathcal{F} : \|f - f_0\|_n \geq \widetilde{M}_1 \epsilon_n | \mathbf{Y}\right) \rightarrow 0 \text{ a.s. } \widetilde{\mathbb{P}}_0 \text{ as } n, p \rightarrow \infty, \quad (6.11)$$

$$\Pi\left(\sigma^2 : |\sigma^2 - \sigma_0^2| \geq 4\sigma_0^2 \epsilon_n | \mathbf{Y}\right) \rightarrow 0 \text{ as } n \rightarrow \infty, \text{ a.s. } \widetilde{\mathbb{P}}_0 \text{ as } n, p \rightarrow \infty, \quad (6.12)$$

for some $\widetilde{M}_1 > 0$.

Remark 4. *Extension of Theorem 4 to the case with interactions is straightforward. In this case, we now have $p + p(p - 1)/2$ unknown functions to estimate. With suitable modifications to Assumptions (B1)-(B6), the rate under the interaction model is $\epsilon_n = \max\{\sqrt{s_0 \log[p + p(p - 1)/2]/n}, d^{-\kappa}\}$.*

Let the generalized dimensionality $|\gamma(\beta)|$ be defined as before in (6.6) (replacing G with p), with ω_g from (6.7) as the threshold (replacing m_g with d). The next theorem shows that under the NPSSL, the expected posterior probability that the generalized dimension size is a constant multiple larger than the true model size s_0 asymptotically vanishes.

Theorem 5 (dimensionality). *Suppose that Assumptions (B1)-(B6) hold. Further assume that $\lambda_0 = (1 - \theta)/\theta = p^c$ where $c \geq 2$, and $\lambda_1 \asymp 1/n$. Then for sufficiently large $\widetilde{M}_2 > 0$,*

$$\sup_{\beta_0} \widetilde{\mathbb{E}}_{\beta_0} \Pi\left(\beta : |\gamma(\beta)| > \widetilde{M}_2 s_0 | \mathbf{Y}\right) \rightarrow 0 \text{ as } n, p \rightarrow \infty. \quad (6.13)$$

7 Simulation Studies

In this section, we will evaluate our method in a number of settings. For the SSGL approach, we fix $\lambda_1 = 1$ and use cross-validation to choose from

$\lambda_0 \in \{1, 2, \dots, 100\}$. For the prior $\theta \sim \mathcal{B}(a, b)$, we set $a = 1, b = G$ so that θ is small with high probability. We will compare our SSGL approach with the following methods:

1. GroupLasso: the group lasso [53]
2. BSGS: Bayesian sparse group selection [6]
3. SoftBart: soft Bayesian additive regression tree (BART) [23]
4. RandomForest: random forests [5]
5. SuperLearner: super learner [47]
6. GroupSpike: point-mass spike-and-slab priors (1.3) placed on groups of coefficients¹

In our simulations, we will look at the mean squared error (MSE) for estimating $f(\mathbf{X}_{\text{new}})$ averaged over a new sample of data \mathbf{X}_{new} . We will also evaluate the variable selection properties of the different methods using precision and recall, where precision = TP/(TP + FP), recall = TP/(TP + FN), and TP, FP, and FN denote the number of true positives, false positives, and false negatives respectively. Note that we will not show precision or recall for the SuperLearner, which averages over different models and different variable selection procedures and therefore does not have one set of variables that are deemed significant.

7.1 Sparse Semiparametric Regression

Here, we will evaluate the use of our proposed SSGL procedure in sparse semiparametric regression with p continuous covariates. Namely, we implement the NPSSL main effects model described in Section 5.1. In Appendix B, we include more simulation studies of the SSGL approach under both sparse and dense settings, as well as a simulation study showing that we are accurately estimating the residual variance σ^2 .

We let $n = 100, p = 300$. We generate independent covariates from a standard uniform distribution, and we let the true regression surface take the following form:

$$\mathbb{E}(Y|\mathbf{X}) = 5\sin(\pi X_1) + 2.5(X_3^2 - 0.5) + e^{X_4} + 3X_5,$$

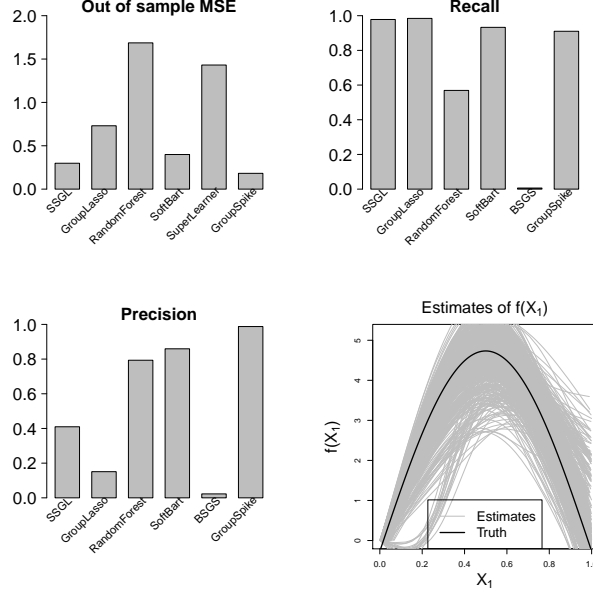


Figure 1: Simulation results for semiparametric regression. The top left panel presents the out-of-sample mean squared error, the top right panel shows the recall score to evaluate variable selection, the bottom left panel shows the precision score, and the bottom right panel shows the estimates from each simulation of $f_1(X_1)$ for SSGL. The MSE for BSGS is not displayed as it lies outside of the plot area.

with variance $\sigma^2 = 1$.

To implement the SSGL approach, we estimate the mean response as

$$\mathbb{E}(Y|\mathbf{X}) = \widetilde{\mathbf{X}}_1\beta_1 + \cdots + \widetilde{\mathbf{X}}_p\beta_p,$$

where $\widetilde{\mathbf{X}}_j$ is a design matrix of basis functions used to capture the possibly nonlinear effect of X_j on Y . For the basis functions in $\widetilde{\mathbf{X}}_j, j = 1, \dots, p$, we use natural splines with degrees of freedom d chosen from $d \in \{2, 3, 4\}$ using cross-validation. Thus, we are estimating a total of between 600 and 1200 unknown basis coefficients.

We run 1000 simulations and average all of the metrics considered over each simulated data set. Figure 1 shows the results from this simulation

¹Code to implement GroupSpike is included in the Supplementary data. Due to the discontinuous prior, GroupSpike is not amenable to a MAP finding algorithm and has to be implemented using MCMC.

study. The GroupSpike approach has the best performance in terms of MSE, followed closely by SSGL, with the next best approach being SoftBart. In terms of recall, the SSGL and GroupLasso approaches perform the best, indicating the highest power in detecting the significant groups. This comes with a loss of precision as the GroupSpike and SoftBart approaches have the best precision among all methods.

Although the GroupSpike method performed best in this scenario, the SSGL method was much faster. As we show in Section B.5 of the Appendix, when $p = 2000$, fitting the SSGL model with a sufficiently large λ_0 takes around three seconds to run. This is almost 50 times faster than running 100 MCMC iterations of the GroupSpike method (never mind the total time it takes for the GroupSpike model to converge). Our experiments demonstrate that the SSGL model gives comparable performance to the “theoretically ideal” point mass spike-and-slab in a fraction of the computational time.

7.2 Interaction detection

We now explore the ability of the SSGL approach to identify important interaction terms in a nonparametric regression model. To this end, we implement the NPSSL model with interactions from Section 5.2. We generate 25 independent covariates from a standard uniform distribution with a sample size of 300. Data is generated from the model:

$$\mathbb{E}(Y|\mathbf{X}) = 2.5\sin(\pi X_1 X_2) + 2\cos(\pi(X_3 + X_5)) + 2(X_6 - 0.5) + 2.5X_7,$$

with variance $\sigma^2 = 1$. While this may not seem like a high-dimensional problem, we will consider all two-way interactions, and there are 300 such interactions. The important two-way interactions are between X_1 and X_2 and between X_3 and X_5 . We evaluate the performance of each method and examine the ability of SSGL to identify important interactions while excluding all of the remaining interactions. Figure 2 shows the results for this simulation setting. The SSGL, GL, GroupSpike, and SoftBart approaches all perform well in terms of out-of-sample mean squared error, with GroupSpike slightly outperforming the competitors. The SSGL also does a very good job at identifying the two important interactions. The (X_1, X_2) interaction is included in 97% of simulations, while the (X_3, X_5) interaction is included 100% of the time. All other interactions are included in only a small fraction of simulated data sets.

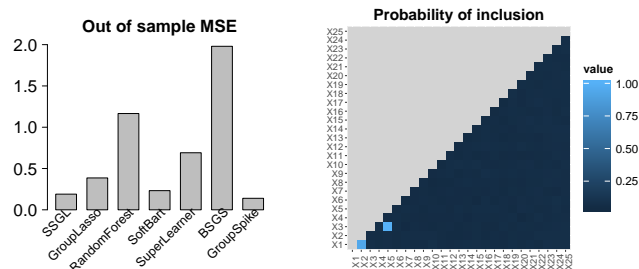


Figure 2: Simulation results from the interaction setting. The left panel shows out-of-sample MSE for each approach, while the right panel shows the probability of a two-way interaction being included into the SSGL model for all pairs of covariates.

8 Real Data Analysis

Here, we will test the SSGL procedure in three distinct settings: 1) comparing its predictive performance against benchmark data sets used in high-dimensional regression, 2) identifying important (nonlinear) main effects and interactions of environmental exposures, and 3) evaluating its performance on a data set where $p \gg n$.

8.1 Testing predictive performance

We first look at three data sets which have been analyzed in a number of manuscripts, most recently in [23]. The tecator data set is available in the `caret` package in R [18] and has three different outcomes \mathbf{Y} to analyze. Specifically, this data set looks at using 100 infrared absorbance spectra to predict three different features of chopped meat with a sample size of 215. The Blood-Brain data is also available in the `caret` package and aims to predict levels of a particular compound in the brain given 134 molecular descriptors with a sample size of 208. Lastly, the Wipp data set contains 300 samples with 30 features from a computer model used to estimate two-phase fluid flow [41]. For each of these data sets, we hold out 20 of the subjects in the data as a validation sample and see how well the model predicts the outcome in the held-out data. We repeat this 1000 times and compute the root mean squared error (RMSE) for prediction.

Table 2 shows the results for each of the methods considered in the simulation study. The results are standardized so that for each data set, the

| Data | SSGL | GroupLasso | RandomForest | SoftBart | SuperLearner | BSGS | GroupSpike |
|------------|------|------------|--------------|----------|--------------|------|------------|
| Tecator 1 | 1.41 | 1.57 | 2.75 | 1.93 | 1.00 | 5.16 | 1.67 |
| Tecator 2 | 1.25 | 1.58 | 2.91 | 1.97 | 1.00 | 6.77 | 1.41 |
| Tecator 3 | 1.14 | 1.38 | 1.94 | 1.81 | 1.10 | 3.31 | 1.00 |
| BloodBrain | 1.10 | 1.04 | 1.00 | 1.01 | 1.00 | 1.24 | 1.13 |
| Wipp | 1.44 | 1.30 | 1.46 | 1.00 | 1.17 | 4.68 | 1.30 |

Table 2: Standardized out-of-sample root mean squared prediction error averaged across 1000 replications for the data sets in Section 8.1. An RMSE of 1 indicates the best performance within a data set.

RMSE is divided by the minimum RMSE for that data set. This means that the model with an RMSE of 1 had the best predictive performance, and all others should be greater than 1, with the magnitude indicating how poor the performance was. We see that the top performer across the data sets was SuperLearner, which is not surprising given that SuperLearner is quite flexible and averages over many different prediction models. Our simulation studies showed that SuperLearner may not work as well when $p > n$. However, the data sets considered here all have $p < n$, which could explain its improved performance here. Among the other approaches, SSGL performs quite well as it has RMSE’s relatively close to 1 for all the data sets considered.

8.2 Environmental exposures in the NHANES data

Here, we analyze data from the 2001-2002 cycle of the National Health and Nutrition Examination Survey (NHANES), which was previously analyzed by Antonelli et al. [1]. We aim to identify which organic pollutants are associated with changes in leukocyte telomere length (LTL) levels. Telomeres are segments of DNA that help to protect chromosomes, and LTL levels are commonly used as a proxy for overall telomere length. LTL levels have previously been shown to be associated with adverse health effects [14], and recent studies within the NHANES data have found that organic pollutants can be associated with telomere length [27].

We use the SSGL approach to evaluate whether any of 18 organic pollutants are associated with LTL length and whether there are any significant interactions among the pollutants also associated with LTL length. In addition to the 18 exposures, there are 18 additional demographic variables which we adjust for in our model. We model the effects of the 18 exposures on LTL length using spline basis functions with 2 degrees of freedom. For the interaction terms, this leads to 4 terms for each pair of interactions, and

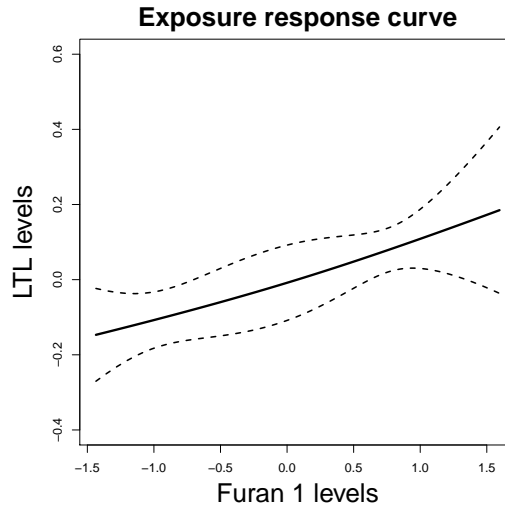


Figure 3: Estimated exposure-response curve between Furan1 and LTL levels in the NHANES data.

we orthogonalize these terms with respect to the main effects. In total, this leads to a data set with $n = 1003$ and $p = 666$.

Our model identifies four main effects and six interaction terms. We will highlight the main effect of the first furan as this group had substantially larger estimated coefficients than the other nonzero groups. The exposure-response curve between this pollutant and LTL levels is shown in Figure 3. There is a positive association between this furan and LTL levels, and this relationship seems to be close to linear, which agrees with a previous analysis of these data that found a similar effect of this furan [1]. Further, our model identifies more main effects and more interactions than previous analyses of these data, which could lead to more targeted future research in understanding how these pollutants affect telomere length.

8.3 Bardet-Biedl syndrome gene expression study

We now analyze a microarray dataset consisting of gene expression measurements from the eye tissue of 120 laboratory rats². The data was originally studied by Scheetz et al. [37] to investigate mammalian eye disease, and later analyzed by Breheny and Huang [4] to demonstrate the performance of their

²Data accessed from the Gene Expression Omnibus www.ncbi.nlm.nih.gov/geo (accession no. GSE5680).

| | SSGL | Group Lasso |
|-------------------|---------------|---------------|
| # groups selected | 13 | 65 |
| 10-fold CV error | 0.012 (0.003) | 0.016 (0.007) |

Table 3: Results for SSGL and Group Lasso on the Bardet-Biedl syndrome gene expression dataset. In parentheses, we report the standard errors for the CV prediction error.

group variable selection algorithm. In this data, the goal is to identify genes which are associated with the gene TRIM32. TRIM32 has previously been shown to cause Bardet-Biedl syndrome [7], a disease affecting multiple organs including the retina.

The original data consists of 31,099 probe sets. Following Breheny and Huang [4], we included only the 5,000 probe sets with the largest variances in expression (on the log scale). For these probe sets, we considered a three-term natural cubic spline basis expansion, resulting in a grouped regression problem with $n = 120$ and $p = 15,000$. We implemented SSGL with regularization parameter values $\lambda_1 = 1$ and λ_0 ranging on an equally spaced grid from 1 to 500. We compared SSGL with the Group Lasso [53], implemented using the R package `gglasso` [51].

As shown in Table 3, SSGL selected much fewer groups than the group lasso. Namely, SSGL selected 13 probe sets, while group lasso selected 65 probe sets. Moreover, SSGL achieved a smaller 10-fold cross-validation error than the group lasso, albeit within range of random variability (Table 3). These results demonstrate that the SSGL achieves strong predictive accuracy, while *also* achieving the most parsimony.

9 Discussion

We have introduced the spike-and-slab group lasso (SSGL) model for variable selection and linear regression with grouped variables. We also extended the SSGL model to generalized additive models with the nonparametric spike-and-slab lasso (NPSSL). The NPSSL can efficiently identify both non-linear main effects *and* higher-order nonlinear interaction terms. Moreover, our prior performs an automatic multiplicity adjustment and self-adapts to the true sparsity pattern of the data through a *non*-separable penalty. For computation, we introduced highly efficient coordinate ascent algorithms for MAP estimation and employed de-biasing methods for uncertainty quantification. An R package implementing the SSGL model can be found at

<https://github.com/jantonelli111/SSGL>.

Although our model performs group selection, it does so in an “all-in-all-out” manner, similar to the original group lasso [53]. Future work will be to extend our model to perform both group selection and within-group selection of individual coordinates. We are currently working to extend the SSGL to perform bilevel selection.

We are also working to extend the nonparametric spike-and-slab lasso so it can adapt to even more flexible regression surfaces than the generalized additive model. Under the NPSSL model, we used cross-validation to tune a single value for the degrees of freedom. In reality, different functions can have vastly differing degrees of smoothness, and it will be desirable to model anisotropic regression surfaces while avoiding the computational burden of tuning the individual degrees of freedom over a p -dimensional grid.

Acknowledgments

Dr. Ray Bai, Dr. Gemma Moran, and Dr. Joseph Antonelli contributed equally and wrote this manuscript together, with input and suggestions from all other listed co-authors. Dr. Ray Bai and Dr. Mary Boland were funded in part by generous funding from the Perelman School of Medicine, University of Pennsylvania. Dr. Ray Bai and Dr. Yong Chen were funded by NIH grants 1R01AI130460 and 1R01LM012607. The authors would like to thank Ruoyang Zhang, Peter Bühlmann, and Edward George for helpful discussions. The authors are also grateful to three anonymous reviewers whose thoughtful comments and suggestions helped to improve this manuscript.

References

- [1] Antonelli, J., Mazumdar, M., Bellinger, D., Christiani, D. C., Wright, R., and Coull, B. A. (2017). Estimating the health effects of environmental mixtures using Bayesian semiparametric regression and sparsity inducing priors. *arXiv preprint arXiv:1711.11239*.
- [2] Antonelli, J., Parmigiani, G., and Dominici, F. (2019). High-dimensional confounding adjustment using continuous spike and slab priors. *Bayesian Analysis*, 14(3):805–828.
- [3] Bhattacharya, A., Pati, D., Pillai, N. S., and Dunson, D. B. (2015). Dirichlet–Laplace priors for optimal shrinkage. *Journal of the American Statistical Association*, 110(512):1479–1490.

- [4] Breheny, P. and Huang, J. (2015). Group descent algorithms for non-convex penalized linear and logistic regression models with grouped predictors. *Statistics and Computing*, 25(2):173–187.
- [5] Breiman, L. (2001). Random forests. *Machine Learning*, 45(1):5–32.
- [6] Chen, R.-B., Chu, C.-H., Yuan, S., and Wu, Y. N. (2016). Bayesian sparse group selection. *Journal of Computational and Graphical Statistics*, 25(3):665–683.
- [7] Chiang, A. P., Beck, J. S., Yen, H.-J., Tayeh, M. K., Scheetz, T. E., Swiderski, R. E., Nishimura, D. Y., Braun, T. A., Kim, K.-Y. A., Huang, J., et al. (2006). Homozygosity mapping with snp arrays identifies trim32, an e3 ubiquitin ligase, as a bardet–biedl syndrome gene (bbs11). *Proceedings of the National Academy of Sciences*, 103(16):6287–6292.
- [8] De Boor, C. (2001). *A practical guide to splines; rev. ed.* Applied Mathematical Sciences. Springer, Berlin.
- [9] Deshpande, S. K., Ročková, V., and George, E. I. (2018). Simultaneous variable and covariance selection with the multivariate spike-and-slab lasso. *Journal of Computational and Graphical Statistics (to appear)*.
- [10] Friedman, J., Hastie, T., and Tibshirani, R. (2010). Regularization paths for generalized linear models via coordinate descent. *Journal of Statistical Software*, 33(1):1–22.
- [11] Gan, L., Narisetty, N. N., and Liang, F. (2018). Bayesian regularization for graphical models with unequal shrinkage. *Journal of the American Statistical Association (to appear)*.
- [12] Ghosal, S., Ghosh, J. K., and van der Vaart, A. W. (2000). Convergence rates of posterior distributions. *The Annals of Statistics*, 28(2):500–531.
- [13] Ghosal, S. and van der Vaart, A. (2017). *Fundamentals of Nonparametric Bayesian Inference*. Cambridge Series in Statistical and Probabilistic Mathematics. Cambridge University Press.
- [14] Haycock, P. C., Heydon, E. E., Kaptoge, S., Butterworth, A. S., Thompson, A., and Willeit, P. (2014). Leucocyte telomere length and risk of cardiovascular disease: systematic review and meta-analysis. *Bmj*, 349:g4227.

- [15] Huang, J., Breheny, P., and Ma, S. (2012). A selective review of group selection in high-dimensional models. *Statistical science: a review journal of the Institute of Mathematical Statistics*, 27(4).
- [16] Jacob, L., Obozinski, G., and Vert, J.-P. (2009). Group lasso with overlap and graph lasso. In *Proceedings of the 26th Annual International Conference on Machine Learning, ICML '09*, pages 433–440, New York, NY, USA. ACM.
- [17] Javanmard, A. and Montanari, A. (2018). Debiasing the lasso: Optimal sample size for Gaussian designs. *The Annals of Statistics*, 46(6A):2593–2622.
- [18] Kuhn, M. (2008). Building predictive models in R using the caret package. *Journal of Statistical Software*, 28(5):1–26.
- [19] Kyung, M., Gill, J., Ghosh, M., and Casella, G. (2010). Penalized regression, standard errors, and Bayesian lassos. *Bayesian Analysis*, 5(2):369–411.
- [20] Li, Y., Nan, B., and Zhu, J. (2015). Multivariate sparse group lasso for the multivariate multiple linear regression with an arbitrary group structure. *Biometrics*, 71(2):354–363.
- [21] Li, Z., McCormick, T., and Clark, S. (2019). Bayesian joint spike-and-slab graphical lasso. In Chaudhuri, K. and Salakhutdinov, R., editors, *Proceedings of the 36th International Conference on Machine Learning*, volume 97 of *Proceedings of Machine Learning Research*, pages 3877–3885, Long Beach, California, USA. PMLR.
- [22] Lim, M. and Hastie, T. (2015). Learning interactions via hierarchical group-lasso regularization. *Journal of Computational and Graphical Statistics*, 24(3):627–654.
- [23] Linero, A. R. and Yang, Y. (2018). Bayesian regression tree ensembles that adapt to smoothness and sparsity. *Journal of the Royal Statistical Society: Series B (Statistical Methodology)*, 80(5):1087–1110.
- [24] Lique, B., Mengersen, K., Pettitt, A. N., and Sutton, M. (2017). Bayesian variable selection regression of multivariate responses for group data. *Bayesian Analysis*, 12(4):1039–1067.

- [25] Meinshausen, N. and Bühlmann, P. (2006). High-dimensional graphs and variable selection with the lasso. *The Annals of Statistics*, 34(3):1436–1462.
- [26] Mendelson, S. and Pajor, A. (2006). On singular values of matrices with independent rows. *Bernoulli*, 12(5):761–773.
- [27] Mitro, S. D., Birnbaum, L. S., Needham, B. L., and Zota, A. R. (2015). Cross-sectional associations between exposure to persistent organic pollutants and leukocyte telomere length among us adults in nhanes, 2001–2002. *Environmental Health Perspectives*, 124(5):651–658.
- [28] Moran, G. E., Ročková, V., and George, E. I. (2019). Spike-and-slab lasso biclustering. *preprint*.
- [29] Moran, G. E., Ročková, V., and George, E. I. (2018). Variance prior forms for high-dimensional Bayesian variable selection. *Bayesian Analysis (to appear)*.
- [30] Ning, B., Jeong, S., and Ghosal, S. (2018). Bayesian linear regression for multivariate responses under group sparsity. *arXiv pre-print arXiv:1807.03439*.
- [31] Raskutti, G., Wainwright, M. J., and Yu, B. (2010). Restricted eigenvalue properties for correlated gaussian designs. *Journal of Machine Learning Research*, 11:2241–2259.
- [32] Ravikumar, P., Lafferty, J., Liu, H., and Wasserman, L. (2009). Sparse additive models. *Journal of the Royal Statistical Society: Series B (Statistical Methodology)*, 71(5):1009–1030.
- [33] Ročková, V. and George, E. I. (2016). Bayesian penalty mixing: The case of a non-separable penalty. In *Statistical Analysis for High-Dimensional Data: The Abel Symposium 2014*, volume 11, page 233. Springer.
- [34] Ročková, V. (2018). Bayesian estimation of sparse signals with a continuous spike-and-slab prior. *The Annals of Statistics*, 46(1):401–437.
- [35] Ročková, V. and George, E. I. (2016). Fast Bayesian factor analysis via automatic rotations to sparsity. *Journal of the American Statistical Association*, 111(516):1608–1622.

- [36] Ročková, V. and George, E. I. (2018). The spike-and-slab lasso. *Journal of the American Statistical Association*, 113(521):431–444.
- [37] Scheetz, T. E., Kim, K.-Y. A., Swiderski, R. E., Philp, A. R., Braun, T. A., Knudtson, K. L., Dorrance, A. M., DiBona, G. F., Huang, J., Casavant, T. L., et al. (2006). Regulation of gene expression in the mammalian eye and its relevance to eye disease. *Proceedings of the National Academy of Sciences*, 103(39):14429–14434.
- [38] Scott, J. G. and Berger, J. O. (2010). Bayes and empirical-Bayes multiplicity adjustment in the variable-selection problem. *The Annals of Statistics*, 38(5):2587–2619.
- [39] Simon, N., Friedman, J., Hastie, T., and Tibshirani, R. (2013). A sparse-group lasso. *Journal of Computational and Graphical Statistics*, 22(2):231–245.
- [40] Song, Q. and Liang, F. (2017). Nearly optimal Bayesian shrinkage for high dimensional regression. *arXiv pre-print arXiv: 1712.08964*.
- [41] Storlie, C. B., Bondell, H. D., Reich, B. J., and Zhang, H. H. (2011). Surface estimation, variable selection, and the nonparametric oracle property. *Statistica Sinica*, 21(2):679.
- [42] Tang, Z., Shen, Y., Li, Y., Zhang, X., Wen, J., Qian, C., Zhuang, W., Shi, X., and Yi, N. (2018). Group spike-and-slab lasso generalized linear models for disease prediction and associated genes detection by incorporating pathway information. *Bioinformatics*, 34(6):901–910.
- [43] Tang, Z., Shen, Y., Zhang, X., and Yi, N. (2017a). The spike-and-slab lasso Cox model for survival prediction and associated genes detection. *Bioinformatics*, 33(18):2799–2807.
- [44] Tang, Z., Shen, Y., Zhang, X., and Yi, N. (2017b). The spike-and-slab lasso generalized linear models for prediction and associated genes detection. *Genetics*, 205(1):77–88.
- [45] Tibshirani, R. (1996). Regression shrinkage and selection via the lasso. *Journal of the Royal Statistical Society: Series B (Statistical Methodology)*, 58:267–288.
- [46] van de Geer, S., Bühlmann, P., Ritov, Y., and Dezeure, R. (2014). On asymptotically optimal confidence regions and tests for high-dimensional models. *The Annals of Statistics*, 42(3):1166–1202.

- [47] van der Laan, M. J., Polley, E. C., and Hubbard, A. E. (2007). Super learner. *Statistical Applications in Genetics and Molecular Biology*, 6(1):1544–6115.
- [48] Wei, R., Reich, B. J., Hoppin, J. A., and Ghosal, S. (2018). Sparse Bayesian additive nonparametric regression with application to health effects of pesticides mixtures. *Statistica Sinica (to appear)*.
- [49] Xu, X. and Ghosh, M. (2015). Bayesian variable selection and estimation for group lasso. *Bayesian Analysis*, 10(4):909–936.
- [50] Yang, X. and Narisetty, N. N. (2019). Consistent group selection with Bayesian high dimensional modeling. *Bayesian Analysis (to appear)*.
- [51] Yang, Y. and Zou, H. (2015). A fast unified algorithm for solving group-lasso penalize learning problems. *Statistics and Computing*, 25(6):1129–1141.
- [52] Yoo, W. W. and Ghosal, S. (2016). Supremum norm posterior contraction and credible sets for nonparametric multivariate regression. *The Annals of Statistics*, 44(3):1069–1102.
- [53] Yuan, M. and Lin, Y. (2006). Model selection and estimation in regression with grouped variables. *Journal of the Royal Statistical Society: Series B (Statistical Methodology)*, 68(1):49–67.
- [54] Zhang, C.-H. and Zhang, T. (2012). A general theory of concave regularization for high-dimensional sparse estimation problems. *Statistical Science*, 27(4):576–593.

A Additional Computational Details

A.1 Tuning Hyperparameters and Updating the Variance in Algorithm 1

We keep the slab hyperparameter λ_1 fixed at a small value. We have found that our results are not very sensitive to the choice of λ_1 . This parameter controls the variance of the slab component of the prior, and the variance must simply be large enough to avoid overshrinkage of important covariates. For the default implementation, we recommend fixing $\lambda_1 = 1$. This applies minimal shrinkage to the significant groups of coefficients and affords these groups the ability to escape the pull of the spike.

Meanwhile, we choose the spike parameter λ_0 from an increasing ladder of values. We recommend selecting $\lambda_0 \in \{1, 2, \dots, 100\}$, which represents a range from hardly any penalization to very strong penalization. Below, we describe precisely how to tune λ_0 . To account for potentially different group sizes, we use the same λ_0 for all groups but multiply λ_0 by $\sqrt{m_g}$ for each g th group, $g = 1, \dots, G$. As discussed in [4], further scaling of the penalty by group size is necessary in order to ensure that the same degree of penalization is applied to potentially different sized groups. Otherwise, larger groups may be erroneously selected simply because they are larger (and thus have larger ℓ_2 norm), not because they contain significant entries.

When the spike parameter λ_0 is very large, the continuous spike density approximates the point-mass spike. Consequently, we face the computational challenge of navigating a highly multimodal posterior. To ameliorate this problem for the spike-and-slab lasso, Ročková and George [36] recommend a “dynamic posterior exploration” strategy in which the slab parameter λ_1 is held fixed at a small value and λ_0 is gradually increased along a grid of values. Using the solution from a previous λ_0 as a “warm start” allows the procedure to more easily find optimal modes. In particular, when $(\lambda_1 - \lambda_0)^2 \leq 4$, the posterior is convex.

Moran et al. [29] modify this strategy for the unknown σ^2 case. This is because the posterior is always non-convex when σ^2 is unknown. Namely, when $p \gg n$ and $\lambda_0 \approx \lambda_1$, the model can become saturated, causing the residual variance to go to zero. To avoid this suboptimal mode at $\sigma^2 = 0$, Moran et al. [29] recommend fixing σ^2 until the λ_0 value at which the algorithm starts to converge in less than 100 iterations. Then, β and σ^2 are simultaneously updated for the next largest λ_0 in the sequence. The intuition behind this strategy is we first find a solution to the convex problem (in which σ^2 is fixed) and then use this solution as a warm start for the non-convex problem (in which σ^2 can vary).

We pursue a similar “dynamic posterior exploration” strategy with the modification for the unknown variance case for the SSGL in Algorithm 1 of Section 3.3. A key aspect of this algorithm is how to choose the maximum value of λ_0 . Ročková and George [36] recommend this maximum to be the λ_0 value at which the estimated coefficients stabilize. An alternative approach is to choose the maximum λ_0 using cross-validation, a strategy which is made computationally feasible by the speed of our block coordinate ascent algorithm. In our experience, the dynamic posterior exploration strategy favors more parsimonious models than cross-validation. In the simulation studies in Section 7, we utilize cross-validation to choose λ_0 , as there, our primary goal is predictive accuracy rather than parsimony.

A.2 Additional Details for the Inference Procedure

Here, we describe the nodewise regression procedure for estimating $\hat{\Theta}$ in Section 4. This approach for estimating the inverse of the covariance matrix $\hat{\Sigma} = \mathbf{X}^T \mathbf{X}/n$ was originally proposed and studied theoretically in [25] and [46].

For each $j = 1, \dots, p$, let \mathbf{X}_j denote the j th column of \mathbf{X} and \mathbf{X}_{-j} denote the submatrix of \mathbf{X} with the j th column removed. Define $\hat{\gamma}_j$ as

$$\hat{\gamma}_j = \arg \min_{\gamma} (\|\mathbf{X}_j - \mathbf{X}_{-j}\gamma\|_2^2/n + 2\lambda_j \|\gamma\|_1).$$

Now we can define the components of $\hat{\gamma}_j$ as $\hat{\gamma}_{j,k}$ for $k = 1, \dots, p$ and $k \neq j$, and create the following matrix:

$$\hat{\mathbf{C}} = \begin{pmatrix} 1 & -\hat{\gamma}_{1,2} & \dots & -\hat{\gamma}_{1,p} \\ -\hat{\gamma}_{2,1} & 1 & \dots & -\hat{\gamma}_{2,p} \\ \vdots & \vdots & \ddots & \vdots \\ -\hat{\gamma}_{p,1} & -\hat{\gamma}_{p,2} & \dots & 1 \end{pmatrix}.$$

Lastly, let $\hat{\mathbf{T}}^2 = \text{diag}(\hat{\tau}_1^2, \hat{\tau}_2^2, \dots, \hat{\tau}_p^2)$, where

$$\hat{\tau}_j = \|\mathbf{X}_j - \mathbf{X}_{-j}\hat{\gamma}_j\|_2^2/n + \lambda_j \|\hat{\gamma}_j\|_1.$$

We can proceed with $\hat{\Theta} = \hat{\mathbf{T}}^{-2}\hat{\mathbf{C}}$. This choice is used because it puts an upper bound on $\|\hat{\Sigma}\hat{\Theta}_j^T - \mathbf{e}_j\|_\infty$. Other regression models such as the original spike-and-slab lasso [36] could be used instead of the lasso [45] regressions for each covariate. However, we will proceed with this choice, as it has already been studied theoretically and shown to have the required properties to be able to perform inference for β .

B Additional Simulation Results

Here, we present additional results which include different sample sizes than those seen in the manuscript, assessment of the SSGL procedure under dense settings, estimates of σ^2 , and additional figures.

B.1 Increased Sample Size for Sparse Simulation

Here, we present the same sparse simulation setup as that seen in Section 7.1, though we will increase n from 100 to 300. Figure 4 shows the results and we see that they are very similar to those from the manuscript, except

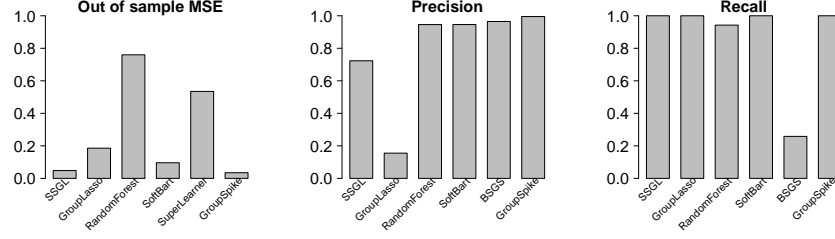


Figure 4: Simulation results from the sparse setting with $n = 300$. The left panel presents the out-of-sample mean squared error, the middle panel shows the precision score, and the right panel shows the recall score. The MSE for BSGS is not displayed as it lies outside of the plot area.

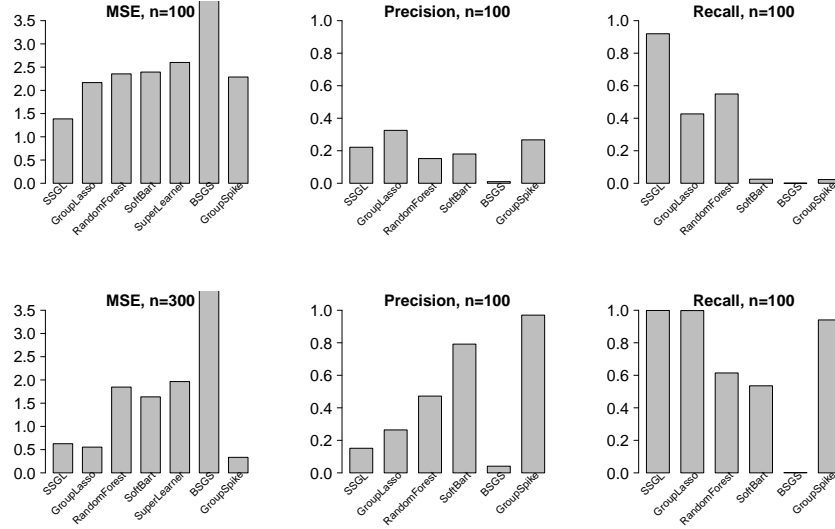


Figure 5: Simulation results from the less sparse setting with $n = 100$ and $n = 300$. The left column shows out-of-sample MSE, the middle panel shows the precision score, and the right column shows the recall score.

that the mean squared error (MSE) for the SSGL approach is now nearly as low as the MSE for the GroupSpike approach, and the precision score has improved substantially.

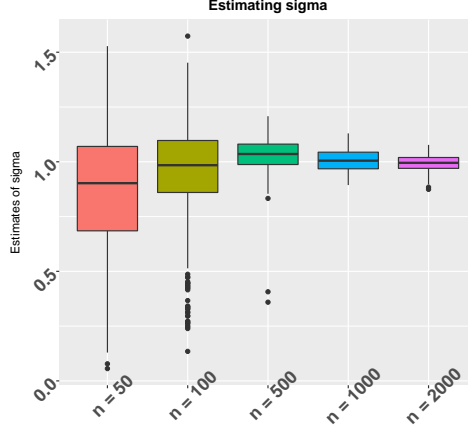


Figure 6: Boxplots of the estimates of σ^2 from the SSGL model for a range of sample sizes. Note that $n = G$ in each scenario.

B.2 Dense Model

Here, we generate independent covariates from a standard normal distribution, and we let the true regression surface take the following form

$$\mathbb{E}(Y|\mathbf{X}) = \sum_{j=1}^{20} 0.2X_j + 0.2X_j^2,$$

with variance $\sigma^2 = 1$. In this model, there are no strong predictors of the outcome, but rather a large number of predictors which have small impacts on the outcome. Here, we display results for both $n = 100$ and $p = 300$, as well as $n = 300$ and $p = 300$, as the qualitative results change across the different sample sizes. Our simulation results can be seen in Figure 5. When the sample size is 100, the SSGL procedure performs the best in terms of both MSE and recall score, while all approaches do poorly with the precision score. When the sample size increases to 300, the SSGL approach still performs quite well in terms of MSE and recall, though the GroupLasso and GroupSpike approaches are slightly better in terms of MSE. The SSGL approach still maintains a low precision score while the GroupSpike approach has a very high precision once the sample size is large enough.

B.3 Estimation of σ^2

To evaluate our ability to estimate σ^2 and confirm our theoretical results that the posterior of σ^2 contracts around the true parameter, we ran a simulation study using the following data generating model:

$$\mathbb{E}(Y|\mathbf{X}) = 0.5X_1 + 0.3X_2 + 0.6X_{10}^2 - 0.2X_{20},$$

with $\sigma^2 = 1$. We vary $n \in \{50, 100, 500, 1000, 2000\}$ and we set $G = n$ to confirm that the estimates are centering around the truth as both the sample size and covariate dimension grows. We use groups of size 2 that contain both the linear and quadratic term for each covariate. Note that in this setting, the total number of regression coefficients actually *exceeds* the sample size since each group has two terms, leading to a total of $p = 2G$ coefficients in the model.

Figure 6 shows box plots of the estimates for σ^2 across all simulations for each sample size and covariate dimension. We see that for small sample sizes there are some estimates well above 1 or far smaller than 1. This is because either some important variables are excluded (so the sum of squared residuals gets inflated), or too many variables are included and the model is overfitted (leading to small $\hat{\sigma}^2$). These problems disappear as the sample size grows to 500 or larger, where we observe that the estimates are closely centering around the true $\sigma^2 = 1$. Figure 6 confirms our theoretical results in Theorem 2 and Theorem 4, which state that as $n, G \rightarrow \infty$, the posterior $\pi(\sigma^2|\mathbf{Y})$ contracts around the true σ^2 .

B.4 Large number of groups

We now generate data with $n = 200$ and $G = 2000$, where each group contains three predictors. We generate data from the following model:

$$\mathbb{E}(\mathbf{Y}|\mathbf{X}) = \sum_{g=1}^G \mathbf{X}_g \boldsymbol{\beta}_g,$$

where we set $\boldsymbol{\beta}_g = \mathbf{0}$ for $g = 1, \dots, 1996$. For the final four groups, we draw individual coefficient values from independent normal distributions with mean 0 and standard deviation 0.4. These coefficients are redrawn for each data set in the simulation study, and therefore, the results are averaging over many possible combinations of magnitudes for the true nonzero coefficients. We see that the best performing approach in this scenario is the GroupSpike approach, followed by the SSGL approach. The SSGL approach outperforms group lasso in terms of MSE and precision, while group lasso has a slightly higher recall score.

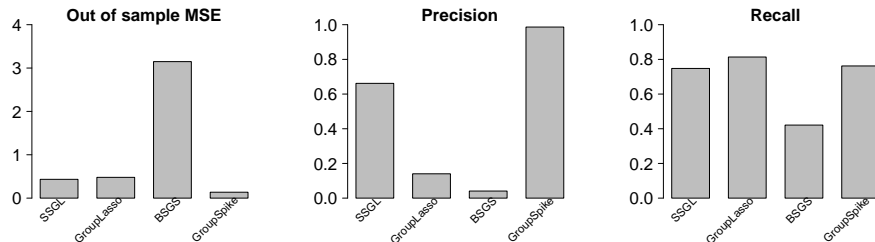


Figure 7: Simulation results from the many groups setting with $G = 2000$. The left panel presents the out-of-sample mean squared error, the middle panel shows the precision score, and the right panel shows the recall score.

B.5 Computation Time

In this study, we evaluate the computational speed of the SSGL procedure in comparison with the fully Bayesian GroupSpike approach that places point-mass spike-and-slab priors on groups of coefficients. We fix $n = 300$ and vary the number of groups $G \in \{100, 200, \dots, 2000\}$. For the SSGL approach, we keep track of the computation time for estimating the model for $\lambda_0 = 20$. For large values of λ_0 , it typically takes 100 or fewer iterations for the SSGL method to converge. For the GroupSpike approach, we keep track of the computation time required to run 100 MCMC iterations. Both SSGL and GroupSpike models were run on an Intel E5-2698v3 processor.

In any given data set, the computation time will be higher than the numbers presented here because the SSGL procedure typically requires fitting the model for multiple values of λ_0 , while the GroupSpike approach will likely take far more than 100 MCMC iterations to converge, especially in higher dimensions. Nonetheless, this should provide a comparison of the relative computation speeds for each approach.

The average CPU time in seconds can be found in Figure 8. We see that the SSGL approach is much faster as it is able to estimate all the model parameters for a chosen λ_0 in just a couple of seconds, even for $G = 2000$. When $G = 2000$, the SSGL returned a final solution in roughly three seconds on average, whereas GroupSpike required over two minutes to run 100 iterations (and would most likely require many more iterations to converge). This is to be expected as the GroupSpike approach relies on MCMC. Figure 8 shows the large computational gains that can be achieved using our MAP finding algorithm.

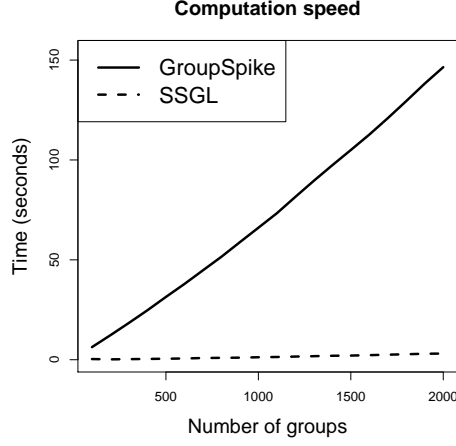


Figure 8: CPU time for the SSGL and GroupSpike approaches averaged across 1000 replications for fixed $n = 300$ and different group sizes G .

C Proofs of Main Results

C.1 Preliminary Lemmas

Before proving the main results in the paper, we first prove the following lemmas.

Lemma 4. *Suppose that $\beta_g \in \mathbb{R}^{m_g}$ follows a group lasso density indexed by λ , i.e. $\beta_g \sim \Psi(\beta_g|\lambda)$. Then*

$$\mathbb{E}(\|\beta_g\|_2^2) = \frac{m_g(m_g + 1)}{\lambda^2}.$$

Proof. The group lasso density, $\Psi(\beta_g|\lambda)$, is the marginal density of a scale mixture,

$$\beta_g \sim \mathcal{N}_{m_g}(\mathbf{0}, \tau \mathbf{I}_{m_g}), \quad \tau \sim \mathcal{G}\left(\frac{m_g + 1}{2}, \frac{\lambda^2}{2}\right).$$

Therefore, using iterated expectations, we have

$$\begin{aligned} \mathbb{E}(\|\beta_g\|_2^2) &= \mathbb{E}\left[\mathbb{E}(\|\beta_g\|_2^2 \mid \tau)\right] \\ &= m_g \mathbb{E}(\tau) \\ &= \frac{m_g(m_g + 1)}{\lambda^2}. \end{aligned}$$

□

Lemma 5. Suppose $\sigma^2 > 0, \sigma_0^2 > 0$. Then for any $\epsilon_n \in (0, 1)$ such that $\epsilon_n \rightarrow 0$ as $n \rightarrow \infty$, we have for sufficiently large n ,

$$\left\{ |\sigma^2 - \sigma_0^2| \geq 4\sigma_0^2\epsilon_n \right\} \subseteq \left\{ \frac{\sigma^2}{\sigma_0^2} > \frac{1 - \epsilon_n}{1 - \epsilon_n} \text{ or } \frac{\sigma^2}{\sigma_0^2} < \frac{1 - \epsilon_n}{1 + \epsilon_n} \right\}.$$

Proof. For large n , $\epsilon_n < 1/2$, so $2\epsilon_n/(1 - \epsilon_n) < 4\epsilon_n$, $-2\epsilon_n/(1 + \epsilon_n) > -4\epsilon_n$, and thus,

$$\begin{aligned} |\sigma^2 - \sigma_0^2| \geq 4\sigma_0^2\epsilon_n &\Rightarrow (\sigma^2 - \sigma_0^2)/\sigma_0^2 \geq 4\epsilon_n \text{ or } (\sigma^2 - \sigma_0^2)/\sigma_0^2 \leq -4\epsilon_n \\ &\Rightarrow \frac{\sigma^2}{\sigma_0^2} - 1 > \frac{2\epsilon_n}{1 - \epsilon_n} \text{ or } \frac{\sigma^2}{\sigma_0^2} - 1 < -\frac{2\epsilon_n}{1 + \epsilon_n} \\ &\Rightarrow \frac{\sigma^2}{\sigma_0^2} > \frac{1 + \epsilon_n}{1 - \epsilon_n} \text{ or } \frac{\sigma^2}{\sigma_0^2} < \frac{1 - \epsilon_n}{1 + \epsilon_n}, \end{aligned}$$

and hence,

$$|\sigma^2 - \sigma_0^2| \geq 4\sigma_0^2\epsilon_n \Rightarrow \frac{\sigma^2}{\sigma_0^2} > \frac{1 + \epsilon_n}{1 - \epsilon_n} \text{ or } \frac{\sigma^2}{\sigma_0^2} < \frac{1 - \epsilon_n}{1 + \epsilon_n}.$$

□

Lemma 6. Suppose that a vector $\mathbf{z} \in \mathbb{R}^m$ can be decomposed into subvectors, $\mathbf{z} = [\mathbf{z}'_1, \dots, \mathbf{z}'_d]$, where $\sum_{i=1}^d |\mathbf{z}_i| = m$ and $|\mathbf{z}_i|$ denotes the length of \mathbf{z}_i . Then $\|\mathbf{z}\|_2 \leq \sum_{i=1}^d \|\mathbf{z}_i\|_2$.

Proof. We have

$$\begin{aligned} \|\mathbf{z}\|_2 &= \sqrt{z_{11}^2 + \dots + z_{1|\mathbf{z}_1|}^2 + \dots + z_{d1}^2 + \dots + z_{d|\mathbf{z}_d|}^2} \\ &\leq \sqrt{z_{11}^2 + \dots + z_{1|\mathbf{z}_1|}^2} + \dots + \sqrt{z_{d1}^2 + \dots + z_{d|\mathbf{z}_d|}^2} \\ &= \|\mathbf{z}_1\|_2 + \dots + \|\mathbf{z}_d\|_2. \end{aligned}$$

□

C.2 Proofs for Section 3

Proof of Proposition 2. This result follows from an adaptation of the arguments of Zhang and Zhang [54]. The group-specific optimization problem is:

$$\hat{\beta}_g = \arg \max_{\beta_g} \left\{ -\frac{1}{2} \|\mathbf{z}_g - \beta_g\|_2^2 + \sigma^2 \text{pen}_S(\beta|\theta) \right\}. \quad (\text{C.1})$$

We first note that the optimization problem (C.1) is equivalent to maximizing the objective

$$L(\beta_g) = -\frac{1}{2}\|z_g - \beta_g\|_2^2 + \sigma^2 \text{pen}_S(\beta|\theta) + \frac{1}{2}\|z_g\|_2^2 \quad (\text{C.2})$$

$$= \|\beta_g\|_2 \left[\frac{\beta_g^T z_g}{\|\beta_g\|_2} - \left(\frac{\|\beta_g\|_2}{2} - \frac{\sigma^2 \text{pen}_S(\beta|\theta)}{\|\beta_g\|_2} \right) \right] \quad (\text{C.3})$$

$$= \|\beta_g\|_2 \left[\|z_g\|_2 \cos \varphi - \left(\frac{\|\beta_g\|_2}{2} - \frac{\sigma^2 \text{pen}_S(\beta|\theta)}{\|\beta_g\|_2} \right) \right] \quad (\text{C.4})$$

where φ is the angle between z_g and β_g . Then, when $\|z_g\|_2 < \Delta$, the second factorized term of (C.4) is always less than zero, and so $\hat{\beta}_g = \mathbf{0}_{m_g}$ must be the global maximizer of L . On the other hand, when the global maximizer $\hat{\beta}_g = \mathbf{0}_{m_g}$, then the second factorized term must always be less than zero, otherwise $\hat{\beta}_g = \mathbf{0}_{m_g}$ would no longer be the global maximizer and so $\|z_g\|_2 < \Delta$. \square

Proof of Lemma 3. We have

$$\mathbb{E}[\theta|\hat{\beta}] = \frac{\int_0^1 \theta^a (1-\theta)^{b-1} (1-\theta z)^{G-\hat{q}} \prod_{g=1}^{\hat{q}} (1-\theta x_g) d\theta}{\int_0^1 \theta^{a-1} (1-\theta)^{b-1} (1-\theta z)^{G-\hat{q}} \prod_{g=1}^{\hat{q}} (1-\theta x_g) d\theta}. \quad (\text{C.5})$$

When $\lambda_0 \rightarrow \infty$, we have $z \rightarrow 1$ and $x_g \rightarrow -\infty$ for all $g = 1, \dots, \hat{q}$. Hence,

$$\lim_{\lambda_0 \rightarrow \infty} \mathbb{E}[\theta|\hat{\beta}] = \lim_{z \rightarrow 1} \lim_{x_g \rightarrow -\infty} \frac{\int_0^1 \theta^a (1-\theta)^{b+G-\hat{q}-1} \prod_{g=1}^{\hat{q}} (1-\theta x_g) d\theta}{\int_0^1 \theta^{a-1} (1-\theta)^{b-1} (1-\theta z)^{G-\hat{q}} \prod_{g=1}^{\hat{q}} (1-\theta x_g) d\theta} \quad (\text{C.6})$$

$$= \frac{\int_0^1 \theta^{a+\hat{q}} (1-\theta)^{b+G-\hat{q}-1} d\theta}{\int_0^1 \theta^{a+\hat{q}-1} (1-\theta)^{b+G-\hat{q}-1} d\theta} \quad (\text{C.7})$$

$$= \frac{a + \hat{q}}{a + b + G}. \quad (\text{C.8})$$

\square

C.3 Proofs for Section 6

In this section, we use proof techniques from [30, 40, 48] rather than the ones in [36]. However, none of these other papers considers *both* continuous spike-and-slab priors for groups of regression coefficients *and* an independent prior on the unknown variance.

Proof of Theorem 2. Our proof is based on first principles of verifying Kullback-Leibler (KL) and testing conditions (see e.g., [12]). We first prove (6.3) and (6.5).

Part I: Kullback-Leibler conditions. Let $f \sim \mathcal{N}_n(\mathbf{X}\boldsymbol{\beta}, \sigma^2 \mathbf{I}_n)$ and $f_0 \sim \mathcal{N}_n(\mathbf{X}\boldsymbol{\beta}_0, \sigma_0^2 \mathbf{I}_n)$, and let $\Pi(\cdot)$ denote the prior (6.2). We first show that for our choice of $\epsilon_n = \sqrt{s_0 \log G/n}$,

$$\Pi\left(K(f_0, f) \leq n\epsilon_n^2, V(f_0, f) \leq n\epsilon_n^2\right) \geq \exp(-C_1 n\epsilon_n^2), \quad (\text{C.9})$$

for some constant $C_1 > 0$, where $K(\cdot, \cdot)$ denotes the KL divergence and $V(\cdot, \cdot)$ denotes the KL variation. The KL divergence between f_0 and f is

$$K(f_0, f) = \frac{1}{2} \left[n \left(\frac{\sigma_0^2}{\sigma^2} \right) - n - n \log \left(\frac{\sigma_0^2}{\sigma^2} \right) + \frac{\|\mathbf{X}(\boldsymbol{\beta} - \boldsymbol{\beta}_0)\|_2^2}{\sigma^2} \right], \quad (\text{C.10})$$

and the KL variation between f_0 and f is

$$V(f_0, f) = \frac{1}{2} \left[n \left(\frac{\sigma_0^2}{\sigma^2} \right)^2 - 2n \left(\frac{\sigma_0^2}{\sigma^2} \right) + n \right] + \frac{\sigma_0^2}{(\sigma^2)^2} \|\mathbf{X}(\boldsymbol{\beta} - \boldsymbol{\beta}_0)\|_2^2. \quad (\text{C.11})$$

Define the two events \mathcal{A}_1 and \mathcal{A}_2 as follows:

$$\mathcal{A}_1 = \left\{ \sigma^2 : n \left(\frac{\sigma_0^2}{\sigma^2} \right) - n - n \log \left(\frac{\sigma_0^2}{\sigma^2} \right) \leq n\epsilon_n^2, \quad n \left(\frac{\sigma_0^2}{\sigma^2} \right)^2 - 2n \left(\frac{\sigma_0^2}{\sigma^2} \right) + n \leq n\epsilon_n^2 \right\} \quad (\text{C.12})$$

and

$$\mathcal{A}_2 = \left\{ (\boldsymbol{\beta}, \sigma^2) : \frac{\|\mathbf{X}(\boldsymbol{\beta} - \boldsymbol{\beta}_0)\|_2^2}{\sigma^2} \leq n\epsilon_n^2, \quad \frac{\sigma_0^2}{(\sigma^2)^2} \|\mathbf{X}(\boldsymbol{\beta} - \boldsymbol{\beta}_0)\|_2^2 \leq n\epsilon_n^2/2 \right\}. \quad (\text{C.13})$$

Following from (C.9)-(C.13), we may write $\Pi(K(f_0, f) \leq \epsilon_n^2, V(f_0, f) \leq \epsilon_n^2) = \Pi(\mathcal{A}_2|\mathcal{A}_1)\Pi(\mathcal{A}_1)$. We derive lower bounds for $\Pi(\mathcal{A}_1)$ and $\Pi(\mathcal{A}_2|\mathcal{A}_1)$ separately. Noting that we may rewrite \mathcal{A}_1 as

$$\mathcal{A}_1 = \left\{ \sigma^2 : \frac{\sigma_0^2}{\sigma^2} - 1 - \log \left(\frac{\sigma_0^2}{\sigma^2} \right) \leq \epsilon_n^2, \quad \left(\frac{\sigma_0^2}{\sigma^2} - 1 \right)^2 \leq \epsilon_n^2 \right\},$$

and expanding $\log(\sigma_0^2/\sigma^2)$ in the powers of $1 - \sigma_0^2/\sigma^2$ to get $\sigma_0^2/\sigma^2 - 1 - \log(\sigma_0^2/\sigma^2) \sim (1 - \sigma_0^2/\sigma^2)^2/2$, it is clear that $\mathcal{A}_1 \supset \mathcal{A}_1^*$, where $\mathcal{A}_1^* = \{\sigma^2 :$

$\sigma_0^2/(\epsilon_n + 1) \leq \sigma^2 \leq \sigma_0^2\}$. Thus, since $\sigma^2 \sim \mathcal{IG}(c_0, d_0)$, we have for sufficiently large n ,

$$\begin{aligned}\Pi(\mathcal{A}_1) &\geq \Pi(\mathcal{A}_1^*) \asymp \int_{\sigma_0^2/(\epsilon_n+1)}^{\sigma_0^2} (\sigma^2)^{-c_0-1} e^{-d_0/\sigma^2} d\sigma^2 \\ &\geq (\sigma_0^2)^{-c_0-1} e^{-d_0(\epsilon_n+1)/\sigma_0^2}.\end{aligned}\tag{C.14}$$

Thus, from (C.14), we have

$$-\log \Pi(\mathcal{A}_1) \lesssim \epsilon_n + 1 \lesssim n\epsilon_n^2,\tag{C.15}$$

since $n\epsilon_n^2 \rightarrow \infty$. Next, we consider $\Pi(\mathcal{A}_2|\mathcal{A}_1)$. We have

$$\frac{\sigma_0^2}{(\sigma^2)^2} \|\mathbf{X}(\boldsymbol{\beta} - \boldsymbol{\beta}_0)\|_2^2 = \left\| \frac{\mathbf{X}(\boldsymbol{\beta} - \boldsymbol{\beta}_0)}{\sigma} \right\|_2^2 \left(\frac{\sigma_0^2}{\sigma^2} - 1 \right) + \left\| \frac{\mathbf{X}(\boldsymbol{\beta} - \boldsymbol{\beta}_0)}{\sigma} \right\|_2^2,$$

and conditional on \mathcal{A}_1 , we have that the previous display is bounded above by

$$\left\| \frac{\mathbf{X}(\boldsymbol{\beta} - \boldsymbol{\beta}_0)}{\sigma} \right\|_2^2 (\epsilon_n + 1) < \frac{2}{\sigma^2} \|\mathbf{X}(\boldsymbol{\beta} - \boldsymbol{\beta}_0)\|_2^2,$$

for large n (since $\epsilon_n < 1$ when n is large). Since $\mathcal{A}_1 \supset \mathcal{A}_1^*$, where \mathcal{A}_1^* was defined earlier, the left-hand side of both expressions in (C.13) can be bounded above by a constant multiple of $\|\mathbf{X}(\boldsymbol{\beta} - \boldsymbol{\beta}_0)\|_2^2$, conditional on \mathcal{A}_1 . Therefore, for some constant $b_1 > 0$, $\Pi(\mathcal{A}_2|\mathcal{A}_1)$ is bounded below by

$$\begin{aligned}\Pi(\mathcal{A}_2|\mathcal{A}_1) &\geq \Pi \left(\|\mathbf{X}(\boldsymbol{\beta} - \boldsymbol{\beta}_0)\|_2^2 \leq \frac{b_1^2 n \epsilon_n^2}{2} \right) \\ &\geq \Pi \left(\|\boldsymbol{\beta} - \boldsymbol{\beta}_0\|_2^2 \leq \frac{b_1^2 \epsilon_n^2}{2kn^{\alpha-1}} \right) \\ &\geq \left\{ \Pi_{S_0} \left(\|\boldsymbol{\beta}_{S_0} - \boldsymbol{\beta}_{0S_0}\|_2^2 \leq \frac{b_1^2 \epsilon_n^2}{4kn^\alpha} \right) \right\} \left\{ \Pi_{S_0^c} \left(\|\boldsymbol{\beta}_{S_0^c}\|_2^2 \leq \frac{b_1^2 \epsilon_n^2}{4kn^\alpha} \right) \right\},\end{aligned}\tag{C.16}$$

where we used Assumption (A3) in the first inequality and the fact that the SSG prior we consider in (6.2) is separable, so $\Pi(\boldsymbol{\beta}) = \Pi_{S_0}(\boldsymbol{\beta})\Pi_{S_0^c}(\boldsymbol{\beta})$. We proceed to bound each bracketed term in (C.16) separately. Changing the variable $\boldsymbol{\beta} - \boldsymbol{\beta}_0 \rightarrow \mathbf{b}$ and using $\Pi_{S_0}(\boldsymbol{\beta}) > \theta^{s_0} \prod_{g \in S_0} [C_g \lambda_1^{m_g} e^{-\lambda_1 \|\boldsymbol{\beta}_g\|_2}]$ and

$\|\mathbf{z}\|_2 \leq \|\mathbf{z}\|_1$ for any vector \mathbf{z} , we have as a lower bound for the first term in (C.16),

$$\theta^{s_0} e^{-\lambda_1 \|\beta_{S_0}\|_2} \prod_{g \in S_0} C_g \left\{ \int_{\|\mathbf{b}_g\|_1 \leq \frac{b_1 \epsilon_n}{2s_0 \sqrt{kn^\alpha}}} \lambda_1^{m_g} e^{-\lambda_1 \|\mathbf{b}_g\|_1} d\mathbf{b}_g \right\}. \quad (\text{C.17})$$

Each of the integral terms in (C.17) is the probability of the first m_g events of a Poisson process happening before time $b_1 \epsilon_n / 2s_0 \sqrt{kn^\alpha}$. Using similar arguments as those in the proof of Lemma 5.1 of [30], we obtain as a lower bound for the product of integrals in (C.17),

$$\begin{aligned} & \prod_{g \in S_0} C_g \left\{ \int_{\|\mathbf{b}_g\|_1 \leq \frac{b_1 \epsilon_n}{2s_0 \sqrt{kn^\alpha}}} \lambda_1^{m_g} e^{-\lambda_1 \|\mathbf{b}_g\|_1} d\mathbf{b}_g \right\} \\ & \geq \prod_{g \in S_0} C_g e^{-\lambda_1 b_1 \epsilon_n / 2s_0 \sqrt{kn^\alpha}} \frac{1}{m_g!} \left(\frac{\lambda_1 b_1 \epsilon_n}{s_0 \sqrt{kn^\alpha}} \right)^{m_g} \\ & = e^{-\lambda_1 b_1 \epsilon_n / 2\sqrt{kn^\alpha}} \prod_{g \in S_0} \frac{C_g}{m_g!} \left(\frac{\lambda_1 b_1 \epsilon_n}{s_0 \sqrt{kn^\alpha}} \right)^{m_g}. \end{aligned} \quad (\text{C.18})$$

Combining (C.17)-(C.18), we have the following lower bound for the first bracketed term in (C.16):

$$\theta^{s_0} e^{-\lambda_1 \|\beta_{S_0}\|_2} e^{-\lambda_1 b_1 \epsilon_n / 2\sqrt{kn^\alpha}} \prod_{g \in S_0} \frac{C_g}{m_g!} \left(\frac{\lambda_1 b_1 \epsilon_n}{s_0 \sqrt{kn^\alpha}} \right)^{m_g}. \quad (\text{C.19})$$

Now, noting that $\Pi_{S_0^c}(\beta) > (1 - \theta)^{G-s_0} \prod_{g \in S_0^c} [C_g \lambda_0^{m_g} e^{-\lambda_0 \|\beta_g\|_2}]$, we further bound the second bracketed term in (C.16) from below. Let $\check{\Pi}(\cdot)$ denote the density, $\check{\Pi}(\beta_g) = C_g \lambda_0^{m_g} e^{-\lambda_0 \|\beta_g\|_2}$. We have

$$\begin{aligned} & \Pi_{S_0^c} \left(\|\beta_{S_0^c}\|_2^2 \leq \frac{b_1^2 \epsilon_n^2}{4kn^\alpha} \right) > (1 - \theta)^{G-s_0} \prod_{g \in S_0^c} \check{\Pi} \left(\|\beta_g\|_2^2 \leq \frac{b_1^2 \epsilon_n^2}{4kn^\alpha (G - s_0)} \right) \\ & \geq (1 - \theta)^{G-s_0} \prod_{g \in S_0^c} \left[1 - \frac{4kn^\alpha (G - s_0) \mathbb{E}_{\check{\Pi}}(\|\beta_g\|_2^2)}{b_1^2 \epsilon_n^2} \right] \\ & = (1 - \theta)^{G-s_0} \prod_{g \in S_0^c} \left[1 - \frac{4kn^\alpha (G - s_0) m_g (m_g + 1)}{\lambda_0^2 b_1^2 \epsilon_n^2} \right] \\ & \geq (1 - \theta)^{G-s_0} \left[1 - \frac{4kn^\alpha G m_{\max} (m_{\max} + 1)}{\lambda_0^2 b_1^2 \epsilon_n^2} \right]^{G-s_0} \end{aligned}$$

$$\asymp (1 - \theta)^{G-s_0} \quad (\text{C.20})$$

where we used an application of the Markov inequality in the second inequality and Lemma 4 in the first equality. The final line of the above display can be verified by recalling that $\lambda_0 = G^c, c \geq 2$ and using our assumptions on m_{\max} in Assumption (A1) and ϵ_n^2 in Theorem 1, and thus, the bracketed term tends to 1 as $n \rightarrow \infty$. Combining (C.19)-(C.20), we obtain for sufficiently large n ,

$$\begin{aligned} -\log \Pi(\mathcal{A}_2|\mathcal{A}_1) &\lesssim s_0 \log \left(\frac{1-\theta}{\theta} \right) - G \log(1-\theta) + \lambda_1 \|\beta_{0S_0}\|_2 + \frac{\lambda_1 b_1 \epsilon_n}{2\sqrt{kn^\alpha}} \\ &\quad + \sum_{g \in S_0} \log(m_g!) - \sum_{g \in S_0} \log C_g + \sum_{g \in S_0} m_g \log \left(\frac{s_0 \sqrt{kn^\alpha}}{\lambda_1 b_1 \epsilon_n} \right). \end{aligned} \quad (\text{C.21})$$

We examine each of the terms in (C.21) separately. Recall that $\lambda_0 = (1 - \theta)/\theta = G^c$ for some $c \geq 2$. Thus, the first term in the above display is bounded above by a constant multiple of $n\epsilon_n^2$. Further, $1 - \theta = \lambda_0/(\lambda_0 + 1) = G^c/(G^c + 1), c \geq 2$, and so the second term in the above display tends to zero as $n \rightarrow \infty$. By Assumptions (A1) and (A5) and the fact that $\lambda_1 \asymp 1/n$, we have

$$\lambda_1 \|\beta_{0S_0}\|_2 \leq \lambda_1 \sqrt{s_0 m_{\max}} \|\beta_{0S_0}\|_\infty \lesssim s_0 \log G \lesssim n\epsilon_n^2,$$

and

$$\frac{\lambda_1 b_1 \epsilon_n}{2\sqrt{kn^\alpha}} \lesssim \epsilon_n \lesssim n\epsilon_n^2.$$

Next, using the facts that $x! \leq x^x$ for $x \in \mathbb{Z}$ and Assumption (A1), we have

$$\sum_{g \in S_0} \log(m_g!) \leq s_0 \log(m_{\max}!) \leq s_0 m_{\max} \log(m_{\max}) \leq s_0 m_{\max} \log n \lesssim n\epsilon_n^2.$$

Using the fact that the normalizing constant, $C_g = 2^{-m_g} \pi^{-(m_g-1)/2} [\Gamma((m_g+1)/2)]^{-1}$, we also have

$$\begin{aligned} \sum_{g \in S_0} -\log C_g &= \sum_{g \in S_0} \left\{ m_g \log 2 + \left(\frac{m_g-1}{2} \right) \log \pi + \log \left[\Gamma \left(\frac{m_g+1}{2} \right) \right] \right\} \\ &\leq s_0 m_{\max} (\log 2 + \log \pi) + \sum_{g \in S_0} \log(m_g!) \\ &\lesssim s_0 m_{\max} (\log 2 + \log \pi) + s_0 m_{\max} \log n \end{aligned}$$

$$\begin{aligned}
&\lesssim s_0 \log G \\
&\lesssim n\epsilon_n^2,
\end{aligned}$$

where we used the fact that $\Gamma((m_g + 1)/2) \leq \Gamma(m_g + 1) = m_g!$. Finally, since $\lambda_1 \asymp 1/n$ and using Assumption (A1) that $m_{\max} = O(\log G / \log n)$, we have

$$\begin{aligned}
\sum_{g \in S_0} m_g \log \left(\frac{s_0 \sqrt{k} n^\alpha}{\lambda_1 b_1 \epsilon_n} \right) &\lesssim s_0 m_{\max} \log \left(\frac{s_0 n^{\alpha/2+1} \sqrt{k}}{b_1 \epsilon_n^2} \right) \\
&= s_0 m_{\max} \log \left(\frac{n^{\alpha/2+2} \sqrt{k}}{b_1 \log G} \right) \\
&\lesssim s_0 m_{\max} \log n \\
&\lesssim s_0 \log G \\
&\lesssim n\epsilon_n^2.
\end{aligned}$$

Combining all of the above, together with (C.21), we have

$$-\log \Pi(\mathcal{A}_2 | \mathcal{A}_1) \lesssim n\epsilon_n^2. \quad (\text{C.22})$$

By (C.15) and (C.22), we may choose a large constant $C_1 > 0$, so that

$$\Pi(\mathcal{A}_2 | \mathcal{A}_1) \Pi(\mathcal{A}_1) \gtrsim \exp(-C_1 n\epsilon_n^2/2) \exp(-C_1 n\epsilon_n^2/2) = \exp(-C_1 n\epsilon_n^2),$$

so the Kullback-Leibler condition (C.9) holds.

Part II: Testing conditions. To complete the proof, we show the existence of a sieve \mathcal{F}_n such that

$$\Pi(\mathcal{F}_n^c) \leq \exp(-C_2 n\epsilon_n^2), \quad (\text{C.23})$$

for positive constant $C_2 > C_1 + 2$, where C_1 is the constant from (C.9), and a sequence of test functions $\phi_n \in [0, 1]$ such that

$$\mathbb{E}_{f_0} \phi_n \leq e^{-C_4 n\epsilon_n^2}, \quad (\text{C.24})$$

and

$$\begin{aligned}
f \in \mathcal{F}_n : \quad &\sup_{\|\beta - \beta_0\|_2 \geq (3 + \sqrt{\nu_1})\sigma_0 \epsilon_n,} \mathbb{E}_f(1 - \phi_n) \leq e^{-C_4 n\epsilon_n^2}, \quad (\text{C.25}) \\
&\text{or } |\sigma^2 - \sigma_0^2| \geq 4\sigma_0^2 \epsilon_n
\end{aligned}$$

for some $C_4 > 0$, where ν is from Assumption (A4). Recall that $\omega_g \equiv \omega_g(\lambda_0, \lambda_1, \theta) = \frac{1}{\lambda_0 - \lambda_1} \log \left[\frac{1-\theta}{\theta} \frac{\lambda_0^{m_g}}{\lambda_1^{m_g}} \right]$. Choose $C_3 \geq C_1 + 2 + \log 2$, and consider the sieve,

$$\mathcal{F}_n = \left\{ f : |\gamma(\beta)| \leq C_3 s_0, 0 < \sigma^2 \leq G^{C_3 s_0 / c_0} \right\}, \quad (\text{C.26})$$

where c_0 is from $\mathcal{IG}(c_0, d_0)$ prior on σ^2 and $|\gamma(\beta)|$ denotes the generalized dimensionality (6.6).

We first verify (C.23). We have

$$\Pi(\mathcal{F}_n^c) \leq \Pi(|\gamma(\beta)| > C_3 s_0) + \Pi(\sigma^2 > G^{C_3 s_0 / c_0}). \quad (\text{C.27})$$

We focus on bounding each of the terms in (C.27) separately. Similarly as in the proof of Theorem 6.3 in Ročková and George [36], we have $\Pi(\beta_g) < 2\theta C_g \lambda_1^{m_g} e^{-\lambda_1 \|\beta_g\|_2}$ for all $\|\beta_g\|_2 > \omega_g$. Let $\mathcal{B} = \{\beta : |\gamma(\beta)| > C_3 s_0\}$. We have as an upper bound on the first term in (C.27),

$$\begin{aligned} \int_{\mathcal{B}} \pi(\beta) d\beta &\leq \sum_{S: |S| > C_3 s_0} 2^{|S|} \theta^{|S|} \int_{\|\beta_g\|_2 > \omega_g; g \in S} C_g \lambda_1^{m_g} e^{-\lambda_1 \|\beta_g\|_2} d\beta_S \\ &\quad \times \int_{\|\beta_g\|_2 \leq \omega_g; g \in S^c} \Pi_{S^c}(\beta) d\beta_{S^c} \\ &\lesssim \sum_{S: |S| > C_3 s_0} \theta^{|S|}, \end{aligned} \quad (\text{C.28})$$

where we used the assumption that $\lambda_1 \asymp 1/n$ and the definition of ω_g to bound the first integral term from above by $\prod_{g \in S} (1/n)^{m_g} \leq n^{-|S|}$, and we bounded the second integral term above by 1. By our assumption that $(1-\theta)/\theta = G^c$ we have $\theta < \theta/(1-\theta) = 1/G^c$, for some $c \geq 2$, and thus, we have as an upper bound for (C.28),

$$\begin{aligned} \sum_{k=\lfloor C_3 s_0 \rfloor + 1}^G \binom{G}{k} \left(\frac{1}{G^c} \right)^k &\leq \sum_{k=\lfloor C_3 s_0 \rfloor + 1}^G \left(\frac{eG}{k} \right)^k \left(\frac{1}{G^c} \right)^k \\ &< \sum_{k=\lfloor C_3 s_0 \rfloor + 1}^G \left(\frac{1}{G(\lfloor C_3 s_0 \rfloor + 1)} \right)^k \\ &= \frac{\left(\frac{1}{G(\lfloor C_3 s_0 \rfloor + 1)} \right)^{\lfloor C_3 s_0 \rfloor + 1} - \left(\frac{1}{G(\lfloor C_3 s_0 \rfloor + 1)} \right)^{G+1}}{1 - \frac{1}{G(\lfloor C_3 s_0 \rfloor + 1)}} \\ &\lesssim G^{-(\lfloor C_3 s_0 \rfloor + 1)} \end{aligned}$$

$$\lesssim \exp\left(-C_3 n \epsilon_n^2\right). \quad (\text{C.29})$$

Next, we have

$$\begin{aligned} \Pi\left(\sigma^2 > G^{C_3 s_0/c_0}\right) &= \int_{G^{C_3 s_0/c_0}}^{\infty} \frac{d_0^{c_0}}{\Gamma(c_0)} (\sigma^2)^{-c_0-1} e^{-d_0/\sigma^2} d\sigma^2 \\ &\lesssim \int_{G^{C_3 s_0/c_0}}^{\infty} (\sigma^2)^{-c_0-1} \\ &\asymp G^{-C_3 s_0} \\ &\lesssim \exp(-C_3 n \epsilon_n^2). \end{aligned} \quad (\text{C.30})$$

Combining (C.28)-(C.30), we have

$$\Pi(\mathcal{F}_n^c) \leq 2 \exp\left(-C_3 n \epsilon_n^2\right) = \exp\left(-C_3 n \epsilon_n^2 + \log 2\right),$$

and so given our choice of C_3 , (C.27) is asymptotically bounded from above by $\exp(-C_2 n \epsilon_n^2)$ for some $C_2 \geq C_1 + 2$. This proves (C.23).

We now proceed to prove (C.24). Our proof is based on the technique used in Song and Liang [40] with suitable modifications. For $\xi \subset \{1, \dots, G\}$, let \mathbf{X}_ξ denote the submatrix of \mathbf{X} with submatrices indexed by ξ , where $|\xi| \leq \bar{p}$ and \bar{p} is from Assumption (A4). Let $\hat{\beta}_\xi = (\mathbf{X}_\xi^T \mathbf{X}_\xi)^{-1} \mathbf{X}_\xi^T \mathbf{Y}$ and $\beta_{0\xi}$ denote the subvector of β_0 with groups indexed by ξ . Let $m_\xi = \sum_{g \in \xi} m_g$, and let $\hat{\sigma}_\xi^2 = \|\mathbf{Y} - \mathbf{X}_\xi \hat{\beta}_\xi\|_2^2 / (n - m_\xi)$. Note that $\hat{\beta}_\xi$ and $\hat{\sigma}_\xi^2$ both exist and are unique because of Assumptions (A1), (A2), and (A4) (which combined, gives us that $m_\xi = o(n)$).

Let \tilde{p} be an integer satisfying $\tilde{p} \asymp s_0$ and $\tilde{p} \leq \bar{p} - s_0$, where \bar{p} is from Assumption (A4), and the specific choice of \tilde{p} will be given below. Recall that S_0 is the set of true nonzero groups with cardinality $s_0 = |S_0|$. Similar to [40], we consider the test function $\phi_n = \max\{\phi'_n, \tilde{\phi}_n\}$, where

$$\begin{aligned} \phi'_n &= \max_{\xi \supset S_0, |\xi| \leq \tilde{p}+s_0} 1 \left\{ |\hat{\sigma}_\xi^2 - \sigma_0^2| \geq \sigma_0^2 \epsilon_n \right\}, \quad \text{and} \\ \tilde{\phi}_n &= \max_{\xi \supset S_0, |\xi| \leq \tilde{p}+s_0} 1 \left\{ \|\hat{\beta}_\xi - \beta_{0\xi}\|_2 \geq \sigma_0 \epsilon_n \right\}. \end{aligned} \quad (\text{C.31})$$

Because of Assumption (A4), we have $\tilde{p} \prec n$ and $\tilde{p} \prec n \epsilon_n^2$. Additionally, since $\epsilon_n = o(1)$, we can use almost identical arguments as those used to establish (A.5)-(A.6) in the proof of Theorem A.1 of [40] to show that for any ξ satisfying $\xi \supset S_0, |\xi| \leq \tilde{p}$,

$$\mathbb{E}_{(\beta_0, \sigma_0^2)} 1 \left\{ |\hat{\sigma}_\xi^2 - \sigma_0^2| \geq \sigma_0^2 \epsilon_n \right\} \leq \exp(-c'_4 n \epsilon_n^2),$$

for some constant $\hat{c}_4 > 0$, and for any ξ satisfying $\xi \supset S_0, |\xi| \leq \tilde{p}$,

$$\mathbb{E}_{(\beta_0, \sigma_0^2)} 1 \left\{ \|\hat{\beta}_\xi - \beta_{0\xi}\|_2 \geq \sigma_0 \epsilon_n \right\} \leq \exp(-\tilde{c}_4 n \epsilon_n^2),$$

for some $\tilde{c}_4 > 0$. Using the proof of Theorem A.1 in [40], we may then choose $\tilde{p} = \lfloor \min\{c'_4, \tilde{c}_4\} n \epsilon_n^2 / (2 \log G) \rfloor$, and then

$$\mathbb{E}_{f_0} \phi_n \leq \exp(-\check{c}_4 n \epsilon_n^2), \quad (\text{C.32})$$

for some $\check{c}_4 > 0$. Next, define the set,

$$\mathcal{C} = \left\{ \|\beta - \beta_0\|_2 \geq (3 + \sqrt{\nu_1}) \sigma_0 \epsilon_n \text{ or } \sigma^2 / \sigma_0^2 > (1 + \epsilon_n) / (1 - \epsilon_n) \right. \\ \left. \text{or } \sigma^2 / \sigma_0^2 < (1 - \epsilon_n) / (1 + \epsilon_n) \right\}.$$

By Lemma 5, we have

$$\sup_{f \in \mathcal{F}_n : \begin{array}{l} \|\beta - \beta_0\|_2 \geq (3 + \sqrt{\nu_1}) \sigma_0 \epsilon_n, \\ \text{or } |\sigma^2 - \sigma_0^2| \geq 4 \sigma_0^2 \epsilon_n \end{array}} \mathbb{E}_f(1 - \phi_n) \leq \sup_{f \in \mathcal{F}_n : (\beta, \sigma^2) \in \mathcal{C}} \mathbb{E}_f(1 - \phi_n). \quad (\text{C.33})$$

Similar to [40], we consider $\mathcal{C} \subset \hat{\mathcal{C}} \cup \tilde{\mathcal{C}}$, where

$$\hat{\mathcal{C}} = \{ \sigma^2 / \sigma_0^2 > (1 + \epsilon_n) / (1 - \epsilon_n) \text{ or } \sigma^2 / \sigma_0^2 < (1 - \epsilon_n) / (1 + \epsilon_n) \}, \\ \tilde{\mathcal{C}} = \{ \|\beta - \beta_0\| \geq (3 + \sqrt{\nu_1}) \sigma_0 \epsilon_n \text{ and } \sigma^2 = \sigma_0^2 \},$$

and so an upper bound for (C.33) is

$$\sup_{f \in \mathcal{F}_n : (\beta, \sigma^2) \in \mathcal{C}} \mathbb{E}_f(1 - \phi_n) = \sup_{f \in \mathcal{F}_n : (\beta, \sigma^2) \in \mathcal{C}} \mathbb{E}_f \min\{1 - \phi'_n, 1 - \tilde{\phi}_n\} \\ \leq \max \left\{ \sup_{f \in \mathcal{F}_n : (\beta, \sigma^2) \in \hat{\mathcal{C}}} \mathbb{E}_f(1 - \phi'_n), \sup_{f \in \mathcal{F}_n : (\beta, \sigma^2) \in \tilde{\mathcal{C}}} \mathbb{E}_f(1 - \tilde{\phi}_n) \right\}. \quad (\text{C.34})$$

Let $\tilde{\xi} = \{g : \|\beta_g\|_2 > \omega_g\} \cup S_0$, $m_{\tilde{\xi}} = \sum_{g \in \tilde{\xi}} m_g$, and $\tilde{\xi}^c = \{1, \dots, G\} \setminus \tilde{\xi}$. For any $f \in \mathcal{F}_n$ such that $(\beta, \sigma^2) \in \hat{\mathcal{C}} \cup \tilde{\mathcal{C}}$, we must have then that $|\tilde{\xi}| \leq C_3 s_0 + s_0 \leq \tilde{p}$, by Assumption (A4). Using Assumption (A3) and (C.26), we also have that for $f \in \mathcal{F}_n, (\beta, \sigma^2) \in \hat{\mathcal{C}} \cup \tilde{\mathcal{C}}$,

$$\|\mathbf{X}_{\tilde{\xi}^c} \beta_{\tilde{\xi}^c}\|_2 \leq \sqrt{kn^\alpha} \|\beta_{\tilde{\xi}^c}\|_2 \\ \leq \sqrt{kn^\alpha} \left[(G - |\tilde{\xi}|) \max_{g \in \tilde{\xi}^c} \omega_g \right]$$

$$\begin{aligned}
&\leq \sqrt{kn^\alpha} \left\{ \frac{G}{\lambda_0 - \lambda_1} \log \left[\frac{1 - \theta}{\theta} \left(\frac{\lambda_0}{\lambda_1} \right)^{m_{\max}} \right] \right\} \\
&\lesssim \min\{\sqrt{k}, 1\} \times \sqrt{\nu_1} \sqrt{n} \sigma_0 \epsilon_n,
\end{aligned} \tag{C.35}$$

where ν is from Assumption (A4). In the above display, we used Lemma 6 in the second inequality, while the last inequality follows from our assumptions on $(\theta, \lambda_0, \lambda_1)$ and m_{\max} , so one can show that the bracketed term in the third line is asymptotically bounded from above by $(\log G(c + \log G))/G$, which can be further bounded above by $D\sqrt{\nu_1}\sqrt{n^{1-\alpha}}\sigma_0\epsilon_n$ for large n and any constant $D > 0$. Thus, using nearly identical arguments as those used to prove Part I of Theorem A.1 in [40], we have

$$\begin{aligned}
&\sup_{f \in \mathcal{F}_n: (\beta, \sigma^2) \in \hat{\mathcal{C}}} \mathbb{E}_f(1 - \phi'_n) \\
&\leq \sup_{f \in \mathcal{F}_n: (\beta, \sigma^2) \in \hat{\mathcal{C}}} \Pr \left(|\chi_{n-m_\xi}^2(\zeta) - (n - m_\xi)| \geq (n - m_\xi)\epsilon_n \right) \\
&\leq \exp(-\hat{c}_4 n \epsilon_n^2),
\end{aligned} \tag{C.36}$$

where the noncentrality parameter ζ satisfies $\zeta \leq n\epsilon_n^2\nu_1\sigma_0^2/16\sigma^2$, and the last inequality follows from the fact that the noncentral χ^2 distribution is subexponential and Bernstein's inequality (see Lemmas A.1 and A.2 in [40]).

Using the arguments in Part I of the proof of Theorem A.1 in [40], we also have that for large n ,

$$\begin{aligned}
&\sup_{f \in \mathcal{F}_n: (\beta, \sigma^2) \in \tilde{\mathcal{C}}} \mathbb{E}_f(1 - \tilde{\phi}_n) \\
&\leq \sup_{f \in \mathcal{F}_n: (\beta, \sigma^2) \in \tilde{\mathcal{C}}} \Pr \left(\|(\mathbf{X}_\xi^T \mathbf{X}_\xi)^{-1} \mathbf{X}_\xi^T \boldsymbol{\epsilon}\|_2 \geq \left[\|\beta_\xi - \beta_{0\xi}\|_2 - \sigma_0 \epsilon_n - \right. \right. \\
&\quad \left. \left. \|(\mathbf{X}_\xi^T \mathbf{X}_\xi)^{-1} \mathbf{X}_\xi^T \mathbf{X}_{\xi^c} \beta_{\xi^c}\|_2 \right] / \sigma \right) \\
&\leq \sup_{f \in \mathcal{F}_n: (\beta, \sigma^2) \in \tilde{\mathcal{C}}} \Pr \left(\|(\mathbf{X}_\xi^T \mathbf{X}_\xi)^{-1} \mathbf{X}_\xi^T \boldsymbol{\epsilon}\|_2 \geq \epsilon_n \right) \\
&\leq \sup_{f \in \mathcal{F}_n: (\beta, \sigma^2) \in \tilde{\mathcal{C}}} \Pr(\chi_{|\tilde{\xi}|}^2 \geq n\nu_1 \epsilon_n^2) \\
&\leq \exp(-\tilde{c}_4 n \epsilon_n^2),
\end{aligned} \tag{C.37}$$

where the second inequality in the above display holds since $\|\beta_\xi - \beta_{0\xi}\|_2 \geq \|\beta - \beta_0\|_2 - \|\beta_{\xi^c}\|_2$, and since (C.35) can be further bounded from above by $\sqrt{kn^\alpha}\sqrt{\nu_1}\sigma_0\epsilon_n$ and thus $\|\beta_{\xi^c}\| \leq \sqrt{\nu_1}\sigma_0\epsilon_n$. Therefore, we have for $f \in \mathcal{F}_n, (\beta, \sigma^2) \in \tilde{\mathcal{C}}$,

$$\|\beta_\xi - \beta_{0\xi}\|_2 \geq (3 + \sqrt{\nu_1})\sigma_0\epsilon_n - \sqrt{\nu_1}\sigma_0\epsilon_n = 3\sigma_0\epsilon_n,$$

while by Assumption (A4) and (C.35), we also have

$$\begin{aligned} \|(\mathbf{X}_{\tilde{\xi}}^T \mathbf{X}_{\tilde{\xi}})^{-1} \mathbf{X}_{\tilde{\xi}}^T \mathbf{X}_{\tilde{\xi}c} \boldsymbol{\beta}_{\tilde{\xi}c}\|_2 &\leq \sqrt{\lambda_{\max}((\mathbf{X}_{\tilde{\xi}}^T \mathbf{X}_{\tilde{\xi}})^{-1})} \|\mathbf{X}_{\tilde{\xi}c} \boldsymbol{\beta}_{\tilde{\xi}c}\|_2 \\ &\leq \left(\sqrt{1/n\nu_1}\right) (\sqrt{n\nu_1} \sigma_0 \epsilon_n) = \sigma_0 \epsilon_n, \end{aligned}$$

and then we used the fact that on the set \tilde{C} , $\sigma = \sigma_0$. The last three inequalities in (C.37) follow from Assumption (A4), the fact that $|\tilde{\xi}| \leq \bar{p} \prec n\epsilon_n^2$, and the fact that for all $m > 0$, $\Pr(\chi_m^2 \geq x) \leq \exp(-x/4)$ whenever $x \geq 8m$. Altogether, combining (C.33)-(C.37), we have that

$$\begin{aligned} \sup_{f \in \mathcal{F}_n : \|\boldsymbol{\beta} - \boldsymbol{\beta}_0\|_2 \geq (3 + \sqrt{\nu})\sigma_0 \epsilon_n, \text{ or } |\sigma^2 - \sigma_0^2| \geq 4\sigma_0^2 \epsilon_n} \mathbb{E}_f(1 - \phi_n) &\leq \exp\left(-\min\{\hat{c}_4, \tilde{c}_4\} n \epsilon_n^2\right), \end{aligned} \quad (\text{C.38})$$

where $\hat{c}_4 > 0$ and $\tilde{c}_4 > 0$ are the constants from (C.36) and (C.37).

Now set $C_4 = \min\{\hat{c}_4, \tilde{c}_4, \check{c}_4\}$, where \check{c}_4 is the constant from (C.32). By and (C.32) and (C.38), this choice of C_4 will satisfy both testing conditions (C.24) and (C.25).

Since we have verified (C.9) and (C.23)-(C.25) for $\epsilon_n = \sqrt{s_0 \log G/n}$, we have

$$\Pi\left(\boldsymbol{\beta} : \|\boldsymbol{\beta} - \boldsymbol{\beta}_0\|_2 \geq (3 + \sqrt{\nu})\sigma_0 \epsilon_n \mid \mathbf{Y}\right) \rightarrow 0 \text{ a.s. } \mathbb{P}_0 \text{ as } n, G \rightarrow \infty,$$

and

$$\Pi\left(\sigma^2 : |\sigma^2 - \sigma_0^2| \geq 4\sigma_0^2 \epsilon_n \mid \mathbf{Y}\right) \rightarrow 0 \text{ as } n \rightarrow \infty, \text{ a.s. } \mathbb{P}_0 \text{ as } n, G \rightarrow \infty,$$

i.e. we have proven (6.3) and (6.5).

Part III. Posterior contraction under prediction error loss. The proof is very similar to the proof of (6.3). The only difference is the testing conditions. We use the same sieve \mathcal{F}_n as that in (C.26) so that (C.23) holds, but now, we need to show the existence of a different sequence of test functions $\tau_n \in [0, 1]$ such that

$$\mathbb{E}_{f_0} \tau_n \leq e^{-C_4 n \epsilon_n^2}, \quad (\text{C.39})$$

and

$$\begin{aligned} \sup_{f \in \mathcal{F}_n : \|\mathbf{X}\boldsymbol{\beta} - \mathbf{X}\boldsymbol{\beta}_0\|_2 \geq M_2 \sigma_0 \sqrt{n} \epsilon_n, \text{ or } |\sigma^2 - \sigma_0^2| \geq 4\sigma_0^2 \epsilon_n} \mathbb{E}_f(1 - \tau_n) &\leq e^{-C_4 n \epsilon_n^2}. \end{aligned} \quad (\text{C.40})$$

Let \tilde{p} be the same integer from (C.31) and consider the test function $\tau_n = \max\{\tau'_n, \tilde{\tau}_n\}$, where

$$\begin{aligned}\tau'_n &= \max_{\xi \supset S_0, |\xi| \leq \tilde{p} + s_0} 1 \left\{ |\hat{\sigma}_\xi^2 - \sigma_0^2| \geq \sigma_0^2 \epsilon_n \right\}, \quad \text{and} \\ \tilde{\tau}_n &= \max_{\xi \supset S_0, |\xi| \leq \tilde{p} + s_0} 1 \left\{ \|\mathbf{X}_\xi \hat{\beta}_\xi - \mathbf{X}_\xi \beta_{0\xi}\|_2 \geq \sigma_0 \sqrt{n} \epsilon_n \right\}.\end{aligned}\tag{C.41}$$

Using Assumption (A4) that for any $\xi \subset \{1, \dots, G\}$ such that $|\xi| \leq \bar{p}$, $\lambda_{\max}(\mathbf{X}_\xi^T \mathbf{X}_\xi) \leq n\nu_2$ for some $\nu_2 > 0$, we have that

$$\|\mathbf{X}_\xi \hat{\beta}_\xi - \mathbf{X}_\xi \beta_{0\xi}\|_2 \leq \sqrt{n\nu_2} \|\hat{\beta}_\xi - \beta_{0\xi}\|_2,$$

and so

$$\Pr\left(\|\mathbf{X}_\xi \hat{\beta}_\xi - \mathbf{X}_\xi \beta_{0\xi}\|_2 \geq \sigma_0 \sqrt{n} \epsilon_n\right) \leq \Pr\left(\|\hat{\beta}_\xi - \beta_{0\xi}\|_2 \geq \nu_2^{-1/2} \sigma_0 \epsilon_n\right).$$

Therefore, using similar steps as those in Part II of the proof, we can show that our chosen sequence of tests τ_n satisfies (C.39) and (C.40). We thus arrive at

$$\Pi\left(\beta : \|\beta - \beta_0\|_2 \geq M_2 \sigma_0 \epsilon_n \mid \mathbf{Y}\right) \rightarrow 0 \text{ a.s. } \mathbb{P}_0 \text{ as } n, G \rightarrow \infty,$$

i.e. we have proven (6.4). \square

Proof of Theorem 3. According to Part I of the proof of Theorem 2, we have that for $\epsilon_n = \sqrt{s_0 \log G/n}$,

$$\Pi\left(K(f_0, f) \leq n\epsilon_n^2, V(f_0, f) \leq n\epsilon_n^2\right) \geq \exp\left(-Cn\epsilon_n^2\right)$$

for some $C > 0$. Thus, by Lemma 8.10 of [13], there exist positive constants C_1 and C_2 such that the event,

$$E_n = \left\{ \int \int \frac{f(\mathbf{Y})}{f_0(\mathbf{Y})} d\Pi(\beta) d\Pi(\sigma^2) \geq e^{-C_1 n \epsilon_n^2} \right\}, \tag{C.42}$$

satisfies

$$\mathbb{P}_0(E_n^c) \leq e^{-(1+C_2)n\epsilon_n^2}. \tag{C.43}$$

Define the set $\mathcal{T} = \{\beta : |\gamma(\beta)| \leq C_3 s_0\}$, where we choose $C_3 > 1 + C_2$. We must show that $\mathbb{E}_0 \Pi(\mathcal{T}^c | \mathbf{Y}) \rightarrow 0$ as $n \rightarrow \infty$. The posterior probability $\Pi(\mathcal{T}^c | \mathbf{Y})$ is given by

$$\Pi(\mathcal{T}^c | \mathbf{Y}) = \frac{\int \int_{\mathcal{T}^c} \frac{f(\mathbf{Y})}{f_0(\mathbf{Y})} d\Pi(\beta) d\Pi(\sigma^2)}{\int \int \frac{f(\mathbf{Y})}{f_0(\mathbf{Y})} d\Pi(\beta) d\Pi(\sigma^2)}. \tag{C.44}$$

By (C.43), the denominator of (C.44) is bounded below by $e^{-(1+C_2)n\epsilon_n^2}$. For the numerator of (C.44), we have as an upper bound,

$$\mathbb{E}_0 \left(\int \int_{\mathcal{T}^c} \frac{f(\mathbf{Y})}{f_0(\mathbf{Y})} d\Pi(\boldsymbol{\beta}) \Pi(\sigma^2) \right) \leq \int_{\mathcal{T}^c} d\Pi(\boldsymbol{\beta}) = \Pi(|\gamma(\boldsymbol{\beta})| > C_3 s_0). \quad (\text{C.45})$$

Using the same arguments as (C.28)-(C.29) in the proof of Theorem 2, we can show that

$$\Pi(|\gamma(\boldsymbol{\beta})| > C_3 s_0) \prec e^{-C_3 n \epsilon_n^2}. \quad (\text{C.46})$$

Combining (C.42)-(C.45), we have that

$$\begin{aligned} \mathbb{E}_0 \Pi(\mathcal{T}^c | \mathbf{Y}) &\leq \mathbb{E}_0 \Pi(\mathcal{T}^c | \mathbf{Y}) 1_{E_n} + \mathbb{P}_0(E_n^c) \\ &< \exp\left((1+C_2)n\epsilon_n^2 - C_3 n \epsilon_n^2\right) + o(1) \\ &\rightarrow 0 \text{ as } n, G \rightarrow \infty, \end{aligned}$$

since $C_3 > 1 + C_2$. This proves (6.8). \square

Proof of Theorem 4. Let $f_{0j}(\mathbf{X}_j)$ be an $n \times 1$ vector with i th entry equal to $f_{0j}(X_{ij})$. Note that proving posterior contraction with respect to the empirical norm (6.11) is equivalent to proving that

$$\Pi \left(\boldsymbol{\beta} : \|\widetilde{\mathbf{X}}\boldsymbol{\beta} - \sum_{j=1}^p f_{0j}(\mathbf{X}_j)\|_2 \geq \widetilde{M}_1 \sqrt{n} \epsilon_n \middle| \mathbf{Y} \right) \rightarrow 0 \text{ a.s. } \widetilde{\mathbb{P}}_0 \text{ as } n, p \rightarrow \infty, \quad (\text{C.47})$$

so to prove the theorem, it suffices to prove (C.47). Let $f \sim \mathcal{N}_n(\widetilde{\mathbf{X}}\boldsymbol{\beta}, \sigma^2 \mathbf{I}_n)$ and $f_0 \sim \mathcal{N}_n(\widetilde{\mathbf{X}}\boldsymbol{\beta}_0 + \boldsymbol{\delta}, \sigma_0^2 \mathbf{I}_n)$, and let $\Pi(\cdot)$ denote the prior (6.2). Similar to the proof for Theorem 2, we show that for our choice of $\epsilon_n = \max\{\sqrt{s_0} \log p/n, d^{-\kappa}\}$ and some constant $C_1 > 0$,

$$\Pi \left(K(f_0, f) \leq n\epsilon_n^2, V(f_0, f) \leq n\epsilon_n^2 \right) \geq \exp(-C_1 n \epsilon_n^2), \quad (\text{C.48})$$

and the existence of a sieve \mathcal{F}_n such that

$$\Pi(\mathcal{F}_n^c) \leq \exp(-C_2 n \epsilon_n^2), \quad (\text{C.49})$$

for positive constant $C_2 > C_1 + 2$, and a sequence of test functions $\phi_n \in [0, 1]$ such that

$$\mathbb{E}_{f_0} \phi_n \leq e^{-C_4 n \epsilon_n^2}, \quad (\text{C.50})$$

and

$$f \in \mathcal{F}_n : \sup_{\substack{\|\widetilde{\mathbf{X}}\boldsymbol{\beta} - \sum_{j=1}^p f_{0j}(\mathbf{X}_j)\|_2 \geq \tilde{c}_0 \sigma_0 \sqrt{n} \epsilon_n, \\ \text{or } |\sigma^2 - \sigma_0^2| \geq 4\sigma_0^2 \epsilon_n}} \mathbb{E}_f(1 - \phi_n) \leq e^{-C_4 n \epsilon_n^2}, \quad (\text{C.51})$$

for some $C_4 > 0$ and $\tilde{c}_0 > 0$.

We first verify (C.48). The KL divergence between f_0 and f is

$$K(f_0, f) = \frac{1}{2} \left[n \left(\frac{\sigma_0^2}{\sigma^2} \right) - n - n \log \left(\frac{\sigma_0^2}{\sigma^2} \right) + \frac{\|\widetilde{\mathbf{X}}(\boldsymbol{\beta} - \boldsymbol{\beta}_0) - \boldsymbol{\delta}\|_2^2}{\sigma^2} \right], \quad (\text{C.52})$$

and the KL variation between f_0 and f is

$$V(f_0, f) = \frac{1}{2} \left[n \left(\frac{\sigma_0^2}{\sigma^2} \right)^2 - 2n \left(\frac{\sigma_0^2}{\sigma^2} \right) + n \right] + \frac{\sigma_0^2}{(\sigma^2)^2} \|\widetilde{\mathbf{X}}(\boldsymbol{\beta} - \boldsymbol{\beta}_0) - \boldsymbol{\delta}\|_2^2. \quad (\text{C.53})$$

Define the two events $\tilde{\mathcal{A}}_1$ and $\tilde{\mathcal{A}}_2$ as follows:

$$\tilde{\mathcal{A}}_1 = \left\{ \sigma^2 : n \left(\frac{\sigma_0^2}{\sigma^2} \right) - n - n \log \left(\frac{\sigma_0^2}{\sigma^2} \right) \leq n \epsilon_n^2, \quad n \left(\frac{\sigma_0^2}{\sigma^2} \right)^2 - 2n \left(\frac{\sigma_0^2}{\sigma^2} \right) + n \leq n \epsilon_n^2 \right\} \quad (\text{C.54})$$

and

$$\tilde{\mathcal{A}}_2 = \left\{ (\boldsymbol{\beta}, \sigma^2) : \frac{\|\widetilde{\mathbf{X}}(\boldsymbol{\beta} - \boldsymbol{\beta}_0) - \boldsymbol{\delta}\|_2^2}{\sigma^2} \leq n \epsilon_n^2, \quad \frac{\sigma_0^2}{(\sigma^2)^2} \|\widetilde{\mathbf{X}}(\boldsymbol{\beta} - \boldsymbol{\beta}_0) - \boldsymbol{\delta}\|_2^2 \leq n \epsilon_n^2 / 2 \right\}. \quad (\text{C.55})$$

Following from (C.52)-(C.55), we have $\Pi(K(f_0, f) \leq n \epsilon_n^2, V(f_0, f) \leq n \epsilon_n^2) = \Pi(\tilde{\mathcal{A}}_2 | \tilde{\mathcal{A}}_1) \Pi(\tilde{\mathcal{A}}_1)$. Using the steps we used to prove (C.15) in part I of the proof of Theorem 2, we have

$$\Pi(\tilde{\mathcal{A}}_1) \gtrsim \exp(-\tilde{c}_1 n \epsilon_n^2), \quad (\text{C.56})$$

for some $\tilde{c}_1 > 0$. Following similar reasoning as in the proof of Theorem 2, we also have for some $b_2 > 0$,

$$\Pi(\tilde{\mathcal{A}}_2 | \tilde{\mathcal{A}}_1) \geq \Pi \left(\|\widetilde{\mathbf{X}}(\boldsymbol{\beta} - \boldsymbol{\beta}_0) - \boldsymbol{\delta}\|_2^2 \leq \frac{b_2^2 n \epsilon_n^2}{2} \right). \quad (\text{C.57})$$

Using Assumptions (B3) and (B6), we have

$$\|\widetilde{\mathbf{X}}(\boldsymbol{\beta} - \boldsymbol{\beta}_0) - \boldsymbol{\delta}\|_2^2 \leq \left(\|\widetilde{\mathbf{X}}(\boldsymbol{\beta} - \boldsymbol{\beta}_0)\|_2 + \|\boldsymbol{\delta}\|_2 \right)^2$$

$$\begin{aligned}
&\leq 2\|\widetilde{\mathbf{X}}(\boldsymbol{\beta} - \boldsymbol{\beta}_0)\|_2^2 + 2\|\boldsymbol{\delta}\|_2^2 \\
&\lesssim 2\left(nk_1\|\boldsymbol{\beta} - \boldsymbol{\beta}_0\|_2^2 + \frac{nk_1b_2^2d^{-2\kappa}}{8}\right) \\
&\asymp 2n\left(\|\boldsymbol{\beta} - \boldsymbol{\beta}_0\|_2^2 + \frac{b_2^2d^{-2\kappa}}{8}\right),
\end{aligned}$$

and so (C.57) can be asymptotically lower bounded by

$$\begin{aligned}
&\Pi\left(\|\boldsymbol{\beta} - \boldsymbol{\beta}_0\|_2^2 + \frac{b_2^2d^{-2\kappa}}{8} \leq \frac{b_2^2\epsilon_n^2}{4}\right) \\
&= \Pi\left(\|\boldsymbol{\beta} - \boldsymbol{\beta}_0\|_2^2 \leq \frac{b_2^2}{4}\left(\epsilon_n^2 - \frac{d^{-2\kappa}}{2}\right)\right).
\end{aligned}$$

Using very similar arguments as those used to prove (C.22), this term can also be lower bounded by $\exp(-\hat{c}_1 n \epsilon_n^2)$. Altogether, we have

$$\Pi(\tilde{A}_2|\tilde{A}_1) \gtrsim \exp(-2\hat{c}_1 \epsilon_n^2). \quad (\text{C.58})$$

Combining (C.56) and (C.58), we have that (C.48) holds. To verify (C.49), we choose $C_3 \geq C_1 + 2 + \log 2$ and use the same sieve \mathcal{F}_n as the one we employed in the proof of Theorem 2 (eq. (C.26)), and then (C.49) holds for our choice of \mathcal{F}_n .

Finally, we follow the recipe of Wei et al. [48] and Song and Liang [40] to construct our test function ϕ_n which will satisfy both (C.50) and (C.51). For $\xi \subset \{1, \dots, p\}$, let $\widetilde{\mathbf{X}}_\xi$ denote the submatrix of $\widetilde{\mathbf{X}}$ with submatrices indexed by ξ , where $|\xi| \leq \bar{p}$ and \bar{p} is from Assumption (A4). Let $\widehat{\boldsymbol{\beta}}_\xi = (\widetilde{\mathbf{X}}_\xi^T \widetilde{\mathbf{X}}_\xi)^{-1} \widetilde{\mathbf{X}}_\xi^T \mathbf{Y}$ and $\boldsymbol{\beta}_{0\xi}$ denote the subvector of $\boldsymbol{\beta}_0$ with basis coefficients appearing in ξ . Then the total number of elements in $\widehat{\boldsymbol{\beta}}_\xi$ is $d|\xi|$. Finally, let $\widehat{\sigma}_\xi^2 = \mathbf{Y}^T(\mathbf{I}_n - \mathbf{H}_\xi)\mathbf{Y}/(n - d|\xi|)$, where $\mathbf{H}_\xi = \widetilde{\mathbf{X}}_\xi(\widetilde{\mathbf{X}}_\xi^T \widetilde{\mathbf{X}}_\xi)^{-1} \widetilde{\mathbf{X}}_\xi^T$ is the hat matrix for the subgroup ξ .

Let \tilde{p} be an integer satisfying $\tilde{p} \asymp s_0$ and $\tilde{p} \leq \bar{p} - s_0$, where \bar{p} is from Assumption (B4) and the specific choice for \tilde{p} will be given later. Recall that S_0 is the set of true nonzero groups with cardinality $s_0 = |S_0|$. Similar to [48], we consider the test function, $\phi_n = \max\{\phi'_n, \tilde{\phi}_n\}$, where

$$\begin{aligned}
\phi'_n &= \max_{\xi \supset S_0, |\xi| \leq \tilde{p} + s_0} 1 \left\{ |\widehat{\sigma}_\xi^2 - \sigma_0^2| \geq c'_0 \sigma_0^2 \epsilon_n \right\}, & \text{and} \\
\tilde{\phi}_n &= \max_{\xi \supset S_0, |\xi| \leq \tilde{p} + s_0} 1 \left\{ \left\| \widetilde{\mathbf{X}} \widehat{\boldsymbol{\beta}}_\xi - \sum_{j \in \xi} f_{0j}(\mathbf{X}_j) \right\|_2 \geq \tilde{c}_0 \sigma_0 \sqrt{n} \epsilon_n \right\},
\end{aligned} \quad (\text{C.59})$$

for some positive constants c'_0 and \tilde{c}_0 . Using Assumption (B1) and (B4), we have that for any ξ in our test ϕ_n , $d|\xi| \leq d(\tilde{p} + s) \leq d\tilde{p} \prec n\epsilon_n^2$. Using essentially the same arguments as those in the proof for Theorem 4.1 in [48], we have that for any ξ which satisfies $\xi \supset S_0$ so that $|\xi| \leq \tilde{p} + s_0$,

$$\mathbb{E}_{(\beta_0, \sigma_0^2)} 1 \left\{ |\hat{\sigma}_\xi^2 - \sigma_0^2| \geq c'_0 \epsilon_n \right\} \leq \exp(-c'_4 n \epsilon_n^2), \quad (\text{C.60})$$

for some $c''_0 > 0$. By Assumption (B3), we also have

$$\begin{aligned} \left\| \widetilde{\mathbf{X}} \hat{\boldsymbol{\beta}} - \sum_{j=1}^p f_{0j}(\mathbf{X}_j) \right\|_2 &= \|\widetilde{\mathbf{X}}(\hat{\boldsymbol{\beta}} - \boldsymbol{\beta}_0) - \boldsymbol{\delta}\|_2 \\ &\leq \sqrt{nk_1} \|\hat{\boldsymbol{\beta}} - \boldsymbol{\beta}_0\|_2 + \|\boldsymbol{\delta}\|_2, \end{aligned}$$

and using the fact that $\|\boldsymbol{\delta}\|_2 \lesssim \sqrt{nd}^{-\kappa} \lesssim \tilde{c}_0 \sigma_0 \sqrt{n} \epsilon_n / 2$ (by Assumption (B6)), we have that for any ξ such that $\xi \supset S_0$, $|\xi| \leq \tilde{p} + s_0$,

$$\begin{aligned} \mathbb{E}_{(\beta_0, \sigma_0^2)} 1 \left\{ \left\| \widetilde{\mathbf{X}} \hat{\boldsymbol{\beta}} - \sum_{j=1}^p f_{0j}(\mathbf{X}_j) \right\|_2 \geq \tilde{c}_0 \sigma_0 \sqrt{n} \epsilon_n \right\} \\ \leq \mathbb{E}_{(\beta_0, \sigma_0^2)} \left\{ \|\hat{\boldsymbol{\beta}} - \boldsymbol{\beta}_0\|_2 \geq \tilde{c}_0 \sigma_0 \epsilon_n / 2 \sqrt{k_1} \right\} \\ \leq \exp(-\tilde{c}_4 n \epsilon_n^2), \end{aligned}$$

for some $\tilde{c}_4 > 0$, where we used the proof of Theorem A.1 in [40] to arrive at the final inequality. Again, as in the proof of Theorem A.1 of [40], we choose $\tilde{p} = \lfloor \min\{c'_4, \tilde{c}_4\} n \epsilon_n^2 / (2 \log p) \rfloor$, and then

$$\mathbb{E}_{f_0} \phi_n \leq \exp(-\check{c}_4 n \epsilon_n^2), \quad (\text{C.61})$$

for some $\check{c}_4 > 0$. Next, we define the set,

$$\mathcal{C} = \left\{ \begin{aligned} &\|\widetilde{\mathbf{X}} \hat{\boldsymbol{\beta}} - \sum_{j=1}^p f_{0j}(\mathbf{X}_j)\|_2 \geq \tilde{c}_0 \sigma_0 \sqrt{n} \epsilon_n \text{ or } \sigma^2 / \sigma_0^2 > (1 + \epsilon_n) / (1 - \epsilon_n) \\ &\text{or } \sigma^2 / \sigma_0^2 < (1 - \epsilon_n) / (1 + \epsilon_n) \end{aligned} \right\}.$$

By Lemma 5, we have

$$\begin{aligned} &\sup_{f \in \mathcal{F}_n : \begin{aligned} &\|\widetilde{\mathbf{X}} \hat{\boldsymbol{\beta}} - \sum_{j=1}^p f_{0j}(\mathbf{X}_j)\|_2 \geq \tilde{c}_0 \sigma_0 \sqrt{n} \epsilon_n, \\ &\text{or } |\sigma^2 - \sigma_0^2| \geq 4\sigma_0^2 \epsilon_n \end{aligned}} \mathbb{E}_f (1 - \phi_n) \\ &\leq \sup_{f \in \mathcal{F}_n : (\boldsymbol{\beta}, \sigma^2) \in \mathcal{C}} \mathbb{E}_f (1 - \phi_n). \end{aligned} \quad (\text{C.62})$$

Similar to [40], we consider $\mathcal{C} \subset \hat{\mathcal{C}} \cup \tilde{\mathcal{C}}$, where

$$\begin{aligned}\hat{\mathcal{C}} &= \{\sigma^2/\sigma_0^2 > (1 + \epsilon_n)/(1 - \epsilon_n) \text{ or } \sigma^2/\sigma_0^2 < (1 - \epsilon_n)/(1 + \epsilon_n)\}, \\ \tilde{\mathcal{C}} &= \{\|\tilde{\mathbf{X}}\boldsymbol{\beta} - \sum_{j=1}^p f_{0j}(\mathbf{X}_j)\|_2 \geq \tilde{c}_0\sigma_0\epsilon_n \text{ and } \sigma^2 = \sigma_0^2\},\end{aligned}$$

and so an upper bound for (C.62) is

$$\begin{aligned}\sup_{f \in \mathcal{F}_n: (\boldsymbol{\beta}, \sigma^2) \in \mathcal{C}} \mathbb{E}_f(1 - \phi_n) &= \sup_{f \in \mathcal{F}_n: (\boldsymbol{\beta}, \sigma^2) \in \mathcal{C}} \mathbb{E}_f \min\{1 - \phi'_n, 1 - \tilde{\phi}_n\} \\ &\leq \max \left\{ \sup_{f \in \mathcal{F}_n: (\boldsymbol{\beta}, \sigma^2) \in \hat{\mathcal{C}}} \mathbb{E}_f(1 - \phi'_n), \sup_{f \in \mathcal{F}_n: (\boldsymbol{\beta}, \sigma^2) \in \tilde{\mathcal{C}}} \mathbb{E}_f(1 - \tilde{\phi}_n) \right\}. \quad (\text{C.63})\end{aligned}$$

Using very similar arguments as those used to prove (C.38) in Theorem 2 and using Assumption (B6), so that the bias $\|\boldsymbol{\delta}\|_2 \lesssim \sqrt{nd}^{-\kappa} \lesssim \sqrt{n}\epsilon_n$, we can show that (C.63) can be further bounded from above as

$$\begin{aligned}f \in \mathcal{F}_n : \quad & \sup_{\substack{\|\tilde{\mathbf{X}}\boldsymbol{\beta} - \sum_{j=1}^p f_{0j}(\mathbf{X}_j)\|_2 \geq \tilde{c}_0\sigma_0\sqrt{n}\epsilon_n, \\ \text{or } |\sigma^2 - \sigma_0^2| \geq 4\sigma_0^2\epsilon_n}} \mathbb{E}_f(1 - \phi_n) \\ & \leq \exp\left(-\min\{\hat{c}_4, \tilde{c}_4\}n\epsilon_n^2\right), \quad (\text{C.64})\end{aligned}$$

where $\hat{c}_4 > 0$ and $\tilde{c}_4 > 0$ are the constants from (C.60) and (C.61).

Choose $C_4 = \min\{\check{c}_4, \hat{c}_4, \tilde{c}_4\}$, and we have from (C.61) and (C.64) that (C.50) and (C.51) both hold.

Since we have verified (C.48) and (C.49)-(C.51) for our choice of $\epsilon_n = \max\{\sqrt{s_0 \log p/n}, d^{-\kappa}\}$, it follows that

$$\Pi \left(\boldsymbol{\beta} : \left\| \tilde{\mathbf{X}}\boldsymbol{\beta} - \sum_{j=1}^p f_{0j}(\mathbf{X}_j) \right\|_2 \geq \tilde{c}_0\sigma_0\sqrt{n}\epsilon_n | \mathbf{Y} \right) \rightarrow 0 \text{ a.s. } \tilde{\mathbb{P}}_0 \text{ as } n, p \rightarrow \infty,$$

and

$$\Pi \left(\sigma^2 : |\sigma^2 - \sigma_0^2| \geq 4\sigma_0^2\epsilon_n | \mathbf{Y} \right) \rightarrow 0 \text{ as } n \rightarrow \infty, \text{ a.s. } \tilde{\mathbb{P}}_0 \text{ as } n, p \rightarrow \infty,$$

i.e. we have proven (C.47), or equivalently, (6.11) and (6.12). \square

Proof of Theorem 5. The proof is very similar to the proof of Theorem 3 and is thus omitted. \square